NASA
Technical
Paper
2586

June 1986

Power Cepstrum Technique With Application to Model Helicopter Acoustic Data

R. M. Martin
and C. L. Burley

NASA

NASA
Technical
Paper
2586

1986

Power Cepstrum Technique With Application to Model Helicopter Acoustic Data

R. M. Martin
Langley Research Center
Hampton, Virginia

C. L. Burley
PRC Kentron, Inc.
Hampton, Virginia

National Aeronautics
and Space Administration

**Scientific and Technical
Information Branch**

CONTENTS

SUMMARY

The application of the power cepstrum to measured helicopter-rotor acoustic data is investigated. A previously applied correction to the reconstructed spectrum, which requires prior knowledge of the echo amplitude or path length, is shown to be incorrect. For an exact echoed signal, the amplitude of the cepstrum echo spike at the echo delay time is linearly related to the relative amplitude of the echo in the time domain. It is shown that if the measured spectrum is not entirely from the source signal, the cepstrum will not yield the desired echo characteristics and cepstral aliasing may occur because of the effective sample rate in the frequency domain. In addition, the spectral analysis bandwidth must be less than one-half the echo ripple frequency or cepstral aliasing can occur. The power cepstrum editing technique is a useful tool for removing some of the contamination because of acoustic reflections from measured rotor acoustic spectra. Although the cepstrum editing yields an improved estimate of the free-field spectrum, the correction process is limited by the lack of accurate knowledge of the echo transfer function. An alternate procedure is proposed which allows the complete correction of a contaminated spectrum through the use of both the transfer function of the echo process and the echo delay time, but which does not require editing in the cepstral domain.

1. INTRODUCTION

The concept of the cepstrum was first reported by Bogert, Healy, and Tukey (ref. 1) as a technique for detecting echoed signals in measured time series. Two general cepstral techniques have been used, the power cepstrum and the complex cepstrum. The power cepstrum is defined as the inverse Fourier transform of the natural logarithm of the power spectrum of the signal. The complex cepstrum is defined as the inverse Fourier transform of the complex logarithm of the Fourier transform of the signal. Both techniques make use of the convolution property of the Fourier transform, that a convolution in the time domain can be transformed to a product in the frequency domain. Both techniques also take advantage of a property of the logarithm function, that the logarithm of a product of two terms is equal to the sum of the logarithms of each term alone. One can consider a directly received signal and its echo as a signal convoluted with itself. The power spectrum of this time series is the product of the spectra of the direct signal and its echo. Taking the natural logarithm of the spectrum then separates the product into the sum of two natural logarithm spectra, that of the direct signal and that representing the echo convolution. The unique characteristics of the individual cepstra of the direct signal and that of the echoes can allow editing of the echo contributions in the total cepstrum. Ideally, if the echo cepstrum can be removed, a transformation back to the frequency domain obtains the spectrum of the original direct signal.

Although the power cepstrum technique allows the reconstruction of an uncontaminated power spectrum, it does not maintain phase information, so that the original uncontaminated time series may not be reconstructed. To obtain the original time series, the complex cepstrum must be used. This technique is complicated by the use of the complex logarithm. Since the complex logarithm is a multivalued function, problems of phase discontinuities arise and the phase function must be "unwrapped" before the calculations can proceed.

Over the last 20 years, the power cepstrum and complex cepstrum techniques have been applied to a wide variety of problems: seismic data (ref. 2), underwater signals (ref. 3), voice analysis (refs. 4 and 5), brain wave signals (electroencephalograph (EEG) and visual evoked responses (VER) (refs. 6 to 8)), gearbox fault analysis (ref. 9), jet noise measurements (refs. 10 to 13), hydrophone calibration (ref. 14), reflector transfer functions and reflection coefficients (ref. 15), and internal-combustion-engine exhaust noise (ref. 16). References 17 and 18 give excellent reviews and bibliographies of the previous applications of the power and complex cepstra in addition to good reviews of the theoretical and practical considerations for each method.

The objective of this work is to investigate the application of the power cepstrum technique to the analysis of model-scale helicopter-rotor noise spectra. Model-scale wind tunnel tests designed to study the acoustic radiation of helicopter rotors have been underway over the past two decades. Because of the relatively large size of model-scale rotors (e.g., a 1/5-scale rotor typically has a 3-m diameter), a wind tunnel test must be conducted in a fairly large test chamber. In order to acquire high-quality acoustic measurements, the tests should ideally be performed in an anechoic facility, one in which the test chamber is treated to minimize acoustic reflections which would contaminate the desired measurements. Unfortunately, there are few large-test-section wind tunnels in existence which are both anechoic and suitable for model rotor testing. For this reason, model tests are often performed in tunnels which have less than ideal acoustic qualities, and thus the measured data are contaminated to some degree with acoustic reflections. In addition, acoustic measurements are often made outdoors at airports and heliports, and are thus easily contaminated with reflections. The power cepstrum technique has been successfully applied by two independent researchers to jet noise spectra which were contaminated with ground plane reflections (refs. 10 to 13). Although the technique was successful, this paper reports a minor error in the analyses employed in these previous efforts (refs. 10 and 12). However, the characteristics of jet noise and rotor noise are quite different, as there is a strong low-frequency tonal content in the rotor signal whereas jet noise is considered more broadband or random in nature.

A joint experiment was performed in 1983 in the Langley 4- by 7-Meter Tunnel by NASA, U.S. Army, and Sikorsky Aircraft Company personnel (refs. 19 and 20). This experiment was the first phase of a three-phase program to investigate the interaction noise of main rotors and tail rotors. During the first phase, the noise of a main rotor alone was studied. The Langley 4- by 7-Meter Tunnel was not designed to be an anechoic test facility, and although measures have been taken to improve its characteristics, the acoustic data acquired contain contamination from the test chamber floor and walls. The acoustic qualities of the tunnel environment are addressed in references 20 and 21. The motivation for the research presented herein was to develop and validate a data reduction technique which could improve the accuracy of the measured acoustic data by removing the undesired reflections.

2. THE POWER CEPSTRUM

Theory

One ideal reflection.- Recall the definition of the forward Fourier transform of a general time function $x(t)$ is

$$X(f) = F\{x(t)\} = \int_{-\infty}^{\infty} x(t)\, e^{-i2\pi ft}\, dt \tag{1}$$

and the inverse Fourier transform of $X(f)$ is

$$x(t) = F^{-1}\{X(f)\} = \int_{-\infty}^{\infty} X(f)\, e^{i2\pi ft}\, df \tag{2}$$

To be an exact Fourier transform pair, the integration limits of equations (1) and (2) are infinite. When dealing with a finite amount of discrete data, however, the time integration must be performed over the period T and the frequency integral is valid only to the Nyquist frequency f_N.

The model of an acoustic signal $g(t)$ with one ideal reflection is

$$x(t) = g(t) + \alpha g(t - t_e) \tag{3}$$

where α is a constant and $0 \leq \alpha < 1.0$. As discussed in section 5, the only constraint on the nature of $g(t)$ is that it have a continuous spectrum in the frequency range of interest. The Fourier transform of equation (3) is

$$X(f) = \int_{-\infty}^{\infty} \left[g(t) + \alpha g(t - t_e)\right] e^{-i2\pi ft}\, dt$$

$$= \int_{-\infty}^{\infty} g(t)\, e^{-i2\pi ft}\, dt + \alpha \int_{-\infty}^{\infty} g(t - t_e)\, e^{-i2\pi ft}\, dt$$

Using the substitutions $\theta = t$ and $\theta = t - t_e$ in each integral and the definition

$$G(f) = \int_{-\infty}^{\infty} g(\theta)\, e^{-i2\pi f\theta}\, d\theta \tag{4}$$

we find that

$$X(f) = \left(1 + \alpha\, e^{-i2\pi ft_e}\right) G(f) \tag{5}$$

The power spectrum of $x(t)$ may be defined as

$$|X(f)|^2 = X(f)X^*(f)$$

$$= \left(1 + \alpha\, e^{-i2\pi f t_e}\right)\left(1 + \alpha\, e^{i2\pi f t_e}\right) G(f)G^*(f)$$

$$= \left[1 + \frac{2\alpha}{1 + \alpha^2} \cos(2\pi f t_e)\right](1 + \alpha^2)\, |G(f)|^2 \qquad (6)$$

Note that in the absence of a reflection (i.e., for $\alpha = 0$), $|X(f)|^2 = |G(f)|^2$. Thus, the terms of the first two brackets of equation (6) are due to the presence of the reflection (i.e., the echo). The cosine term causes the characteristic ripple seen in the power spectra of data containing a reflection. To decouple the terms of equation (6), the natural logarithm is used:

$$\ln|X(f)|^2 = \ln\left[1 + \frac{2\alpha}{1 + \alpha^2} \cos(2\pi f t_e)\right] + \ln(1 + \alpha^2) + \ln|G(f)|^2 \qquad (7)$$

To further decouple equation (7), the power series expansion of the natural logarithm

$$\ln(1 + x) = x - \frac{1}{2} x^2 + \frac{1}{3} x^3 - \frac{1}{4} x^4 + \frac{1}{5} x^5 + \ldots$$

which is valid for $|x| < 1$, is applied to the first term of equation (7) because, for $0 \leq \alpha < 1.0$,

$$\left|\frac{2\alpha}{1 + \alpha^2} \cos(2\pi f t_e)\right| < 1$$

Further simplification of the series expansion is obtained by letting

$$\phi = \frac{2\alpha}{1 + \alpha^2}$$

Thus, equation (7) is written as

$$\ln|X(f)|^2 = \ln|G(f)|^2 + \ln(1 + \alpha^2) + \left[\phi \cos(2\pi f t_e)\right.$$

$$\left. - \frac{1}{2} \phi^2 \cos^2(2\pi f t_e) + \frac{1}{3} \phi^3 \cos^3(2\pi f t_e) + \ldots\right] \qquad (8)$$

The power cepstrum is defined as the inverse finite Fourier transform of the natural logarithm of the power spectrum:

$$C_p(\tau) = F^{-1}\{\ln|X(f)|^2\} \tag{9}$$

Note the similarity to the autocorrelation function

$$R_x(\tau) = F^{-1}\left\{\frac{2\pi}{T}\,|X(f)|^2\right\}$$

Through substitution of equation (8) into equation (9) and use of identities relating $(\cos\theta)^n$ to $\cos(n\theta)$, the power cepstrum is found to be

$$C_p(\tau) = \int_{-f_N}^{f_N} \ln\left[|G(f)|^2\right] e^{i2\pi f\tau}\,df + \int_{-f_N}^{f_N} \ln(1+\alpha^2)\, e^{i2\pi f\tau}\,df$$

$$+ \phi \int_{-f_N}^{f_N} \cos(2\pi f t_e)\, e^{i2\pi f\tau}\,df - \frac{1}{2}\phi^2 \int_{-f_N}^{f_N} \frac{1}{2}\left[1 + \cos(4\pi f t_e)\right] e^{i2\pi f\tau}\,df$$

$$+ \frac{1}{3}\phi^3 \int_{-f_N}^{f_N} \frac{1}{4}\left[3\cos(2\pi f t_e) + \cos(6\pi f t_e)\right] e^{i2\pi f\tau}\,df + \ldots \tag{10}$$

A lengthier expansion of this equation, to the tenth power of $\phi\cos(2\pi f t_e)$, is presented in appendix A for completeness and clarity. Here, the first term is simply equal to $C_{pg}(\tau)$, the power cepstrum of the direct signal $g(t)$. To perform the integration of the remaining terms, note that each can be reduced to the integral of $\cos(2\pi n f t_e)\, e^{i2\pi f\tau}$ (where $n = 0, 1, 2, \ldots$) and recall that

$$\int_{-f_N}^{f_N} \cos(n2\pi f t_e)\, e^{i2\pi f\tau}\,df = f_N\left\{\frac{\sin\left[(nt_e - \tau)2\pi f_N\right]}{(nt_e - \tau)2\pi f_N} + \frac{\sin\left[(nt_e + \tau)2\pi f_N\right]}{(nt_e + \tau)2\pi f_N}\right\}$$

$$(n = 0, 1, 2, \ldots)$$

It is interesting to note that if the integration could be performed over infinite limits, the $(\sin x)/x$ functions would become delta functions.

Now equation (10) may be simplified to

$$C_p(\tau) = C_{pg}(\tau) + 2f_N\left[\ln(1 + \alpha^2) - a_0\right]\left[\frac{\sin(2\pi f_N \tau)}{2\pi f_N \tau}\right]$$

$$+ f_N \sum_{n=1}^{\infty} a_n \left\{ \frac{\sin\left[(nt_e - \tau)2\pi f_N\right]}{(nt_e - \tau)2\pi f_N} + \frac{\sin\left[(nt_e + \tau)2\pi f_N\right]}{(nt_e + \tau)2\pi f_N} \right\} \qquad (11)$$

The second term represents a peak at $\tau = 0$, and the third term represents an infinite series of peaks (called "rahmonics"; analogous to harmonics of a frequency) at multiples of the echo delay time t_e with amplitudes ($f_N a_n$) which are related to the ratio α.

The typical shape of the power cepstrum of the direct wave ($C_{pg}(\tau)$ for a general random signal) is shown in figure 1. It is similar in shape to the autocorrelation of a random signal, as we would expect since the cepstrum would be identical to the autocorrelation if the natural logarithm were not used. The presence of reflections in the signal causes the series of spikes (the $(\sin x)/x$ series) in the cepstrum. To remove the reflections, one can remove the spikes at $\pm nt_e$ ($n = 1, 2, 3, \ldots$) by interpolating new values based on the adjacent values.

It can be shown that the coefficient $\ln(1 + \alpha^2) - a_0$ of the second term in equation (11) (the spike at $\tau = 0$) is identically zero. (See appendix A.) Thus, the only contribution at $\tau = 0$ is from $C_{pg}(\tau)$. It should be noted that Syed et al. (ref. 10) used a different series expansion for $\ln(1 + \alpha^2)$ and approximated the series to only the fourth power. He found that the spike at $\tau = 0$ was multiplied by $\ln(1 + \alpha^2) - 4.35\left[(\phi^2/4) + (3\phi^4/32)\right]$ and that this additional term should be removed. However, since there is a large contribution at $\tau = 0$ from $C_{pg}(\tau)$, it is difficult to edit the cepstrum at that location. Thus, he concluded that one should not edit the cepstrum at $\tau = 0$; rather, one should edit only the spikes at $\tau = \pm nt_e$, and when the cepstrum is transformed back to a power spectrum, the additional $\tau = 0$ term because of the echo becomes a constant amplitude correction to be applied to the reconstructed spectrum. This correction would require knowledge of α. However, since this term is actually zero, no amplitude correction is required.

In addition, work reported by Miles, Stevens, and Leininger (ref. 12) concludes that editing of the cepstrum spikes results in "a spectrum due to intensity addition only of the direct and reflected signals." They also found that the coefficient of the $\tau = 0$ spike is related to $\ln(1 + \alpha^2)$ and that knowledge of α would allow a correction to obtain the free-field spectrum. This also is an incorrect conclusion.

Since the second term in equation (11) is actually multiplied by zero, the actual cepstrum is

$$C_p(\tau) = C_{pg}(\tau) + f_N \sum_{n=1}^{\infty} a_n \left\{ \frac{\sin\left[(nt_e - \tau)2\pi f_N\right]}{(nt_e - \tau)2\pi f_N} + \frac{\sin\left[(nt_e + \tau)2\pi f_N\right]}{(nt_e + \tau)2\pi f_N} \right\} \qquad (12)$$

After the $\pm nt_e$ spikes are removed from the cepstrum, the new edited cepstrum $C'_p(\tau)$ is

$$C'_p(\tau) = C_{pg}(\tau) = F^{-1}\{\ln|G(f)|^2\}$$

To find the free-field power spectrum, a Fourier transform is again performed

$$\ln|G(f)|^2 = F\{C'_p(\tau)\}$$

and the exponential function is used

$$|G(f)|^2 = e^{F\{C'_p(\tau)\}} \tag{13}$$

This results in reconstruction of the free-field power spectrum of the original signal and does not require any amplitude corrections or prior knowledge of the echo amplitude.

Though the cepstrum spikes yield information on the delay time of echoes, they may also be used to estimate the relative amplitudes of the echoes. Through the use of equation (10), it can be shown that the coefficient of the first echo spike of the cepstrum (i.e., the coefficient of the $\int \cos(2\pi f\tau_e)\, e^{i2\pi f\tau}\, df$ terms) is $f_N a_1$, where

$$a_1 = \phi + \frac{1}{3}\frac{3}{4}\phi^3 + \frac{1}{5}\frac{10}{16}\phi^5 + \frac{1}{7}\frac{35}{64}\phi^7 + \frac{1}{9}\frac{126}{256}\phi^9 + \cdots \tag{14}$$

with

$$\phi = \frac{2\alpha}{1 + \alpha^2}$$

It can be shown that this is a convergent series for $0 \leq \alpha < 1.0$ (see appendix B), and the series can be rewritten as follows:

$$a_1 = \sum_{j=1}^{\infty} \frac{\phi^{2j-1}(2j-2)!}{2^{2j-2}(j-1)!j!} = 2\alpha \tag{15}$$

If the value of $C_{pg}(\tau)$ is small at t_e (the value of τ for which the first echo spike occurs, i.e., $\tau = t_e$), then the amplitude at t_e should be essentially $2f_N\alpha$. For many functions, $C_{pg}(\tau)$ typically decreases very quickly with increasing τ, so

often this amplitude is valid. Thus, given the cepstrum of a signal, the amplitude of the first echo spike may be used to find the value of the relative amplitude of the reflection.

Two ideal reflections.- The model of an acoustic signal with two ideal reflections is

$$x(t) = g(t) + \alpha g(t - t_1) + \beta g(t - t_2) \tag{16}$$

Using the same approach as for the one-echo case (refer to eq. (6)), we may express the power spectrum of $x(t)$ as

$$|X(f)|^2 = \left\{1 + \frac{2\alpha}{(1 + \alpha^2 + \beta^2)} \cos(2\pi f t_1) + \frac{2\beta}{(1 + \alpha^2 + \beta^2)} \cos(2\pi f t_2) + \frac{2\alpha\beta}{(1 + \alpha^2 + \beta^2)} \cos\left[2\pi f(t_1 - t_2)\right]\right\}(1 + \alpha^2 + \beta^2)\ |G(f)|^2 \tag{17}$$

To decouple the terms of equation (17), the logarithm is used and is approximated by the power series expansion to the third power to produce

$$\ln|X(f)|^2 \approx \ln|G(f)|^2 + 2\alpha \cos(2\pi f t_1) + 2\beta \cos(2\pi f t_2) - \alpha^2 \cos(2\pi f 2t_1) - \beta^2 \cos(2\pi f 2t_2) + \frac{2}{3}\alpha^3 \cos(2\pi f 3t_1) + \frac{2}{3}\beta^3 \cos(2\pi f 3t_2) - 2\alpha\beta \cos\left[2\pi f(t_1 + t_2)\right] + 2\alpha\beta^2 \cos\left[2\pi f(t_1 + 2t_2)\right] + 2\alpha^2\beta \cos\left[2\pi f(2t_1 + t_2)\right]$$

This approximation is only valid when

$$\left|(\alpha + \beta)^2 + 2(\alpha + \beta)\right| < 1$$

Performing the inverse Fourier transform to obtain the power cepstrum results in

$$C_p(\tau) \approx C_{pg}(\tau) + f_N\left[\sum_{n=1}^{\infty} a_n\left\{\frac{\sin[(nt_1 \pm \tau)2\pi f_N]}{(nt_1 \pm \tau)2\pi f_N}\right\}\right.$$

$$+ \sum_{n=1}^{\infty} b_n\left\{\frac{\sin[(nt_2 \pm \tau)2\pi f_N]}{(nt_2 \pm \tau)2\pi f_N}\right\} + \sum_{n=1}^{\infty} c_n\left(\frac{\sin\{[n(t_1 + t_2) \pm \tau]2\pi f_N\}}{[n(t_1 + t_2) \pm \tau]2\pi f_N}\right)$$

$$\left. + \sum_{n=1}^{\infty} d_n\left(\frac{\sin\{[n(t_1 + 2t_2) \pm \tau]2\pi f_N\}}{[n(t_1 + 2t_2) \pm \tau]2\pi f_N}\right) + \sum_{n=1}^{\infty} e_n\left(\frac{\sin\{[n(2t_1 + t_2) \pm \tau]2\pi f_N\}}{[n(2t_1 + t_2) \pm \tau]2\pi f_N}\right)\right] \tag{18}$$

The factor $1 + \alpha^2 + \beta^2$ in equation (17) is cancelled by the a_0 term from the power series expansion of the logarithm, as is found for the one-echo case (appendix A). No attempt has been made to deduce the exact converged values of the coefficients a_n, b_n, c_n, ... $(n > 0)$ as is done for a_1 of the one-echo case. However, this power series approximation shows that

$$a_1 \approx 2\alpha, \quad a_2 \approx -\alpha^2, \quad a_3 \approx \frac{2}{3}\alpha^3, \quad b_1 \approx 2\beta, \quad b_2 \approx -\beta^2,$$

$$b_3 \approx \frac{2}{3}\beta^3, \quad c_1 \approx -2\alpha\beta, \quad d_1 \approx 2\alpha\beta^2, \text{ and } \quad e_1 \approx 2\alpha^2\beta$$

For the two-echo case, the dominant echo spikes occur at t_1, t_2, $2t_1$, $2t_2$, and $t_1 + t_2$, and the amplitudes at t_1 and t_2 are the same as for a one-echo case. No spikes occur at differences in delay times. The rahmonic spikes (those at sums of multiples of t_1 and t_2) are of lesser amplitude, since they are multiplied by powers of α and β and in practical cases α and β are less than unity. Thus, in analogy to the one-echo case, the cepstrum echo-spike amplitudes are linearly related to the actual echo amplitudes.

Numerical Examples

Direct signal.- To illustrate the results of the preceding analysis, a numerical simulation of a transient signal was performed. The sample transient signal has the exponential form

$$x(t) = e^{-k|t-t_1|} \tag{19}$$

The time history, power spectrum, and power cepstrum are shown in figures 2(a) to 2(c). The power cepstra presented in this report are normalized by twice the Nyquist

frequency ($2f_N$), so that the amplitude of the first cepstrum spike represents the relative echo amplitude as shown by equation (15). In addition, the first few points near $\tau = 0$ are not plotted to increase the plot resolution for the cepstrum at large values of τ.

One ideal reflection.- The sample signal with one echo has the form

$$x(t) = e^{-k|t-t_1|} + \alpha\, e^{-k|t-t_2|} \tag{20}$$

This signal and its power spectrum for $\alpha = 0.5$ and $t_e = 0.0018$ sec are shown in figures 3(a) and 3(b). Note the large-amplitude ripple induced in the spectrum, and that the overall level is 1 dB higher than the original signal (fig. 2(b)). Figure 3(c) shows the normalized cepstrum of the signal of equation (20). The quickly decaying $C_{pg}(\tau)$ function is shown near $\tau = 0$, and the spikes at multiples of the echo delay time are clearly shown. The amplitude of the first cepstrum spike of figure 3(c) is 0.50 (with the neighboring cepstrum values nearly zero), which illustrates the equality with the relative echo amplitude of 0.50 proven by equation (15). These spikes are easily removed by linearly interpolating new values based on adjacent cepstrum values. In this case the editing procedure is fairly straightforward, since the cepstrum levels are very small for $\tau > 0.001$ sec, and the data are numerically "clean."

The reconstructed power spectrum is shown in figure 3(d) and is simply the exponential of the forward Fourier transform of the edited cepstrum. This reconstruction is identical to the Fourier transform of the isolated wavelet (fig. 2(b)) and it is clear that the previously used amplitude corrections (refs. 10 and 12) need not be applied to this result. The difference between the contaminated spectrum (fig. 3(b)) and the edited spectrum (fig. 3(d)) is shown in figure 3(e), which clearly shows the sinusoidal nature of the echo contamination.

Two ideal reflections.- To demonstrate the application of the technique to a signal with two echoes, figure 4(a) shows the same wavelet as shown in figure 2(a) with two echoes. Figures 4(b), 4(c), and 4(d) show the power spectrum, power cepstrum, and reconstructed "free-field" power spectrum of this signal. As shown in equation (18), the effect of multiple echoes is to create cepstrum spikes not only at multiples of the echo delay times but also at sums of multiples of the echo delay times. This effect is shown in figure 4(c). The amplitudes of the cepstrum spikes at $\tau = 0.0018$ and 0.0068 sec correlate well with the expected values of $f_N a_1 \approx f_N 2\alpha$ and $f_N b_1 \approx f_N 2\beta$ found from equation (18). The amplitudes of the cepstrum spikes at multiples and sums of multiples of the two echo delay times also correlate well with the approximated values of their coefficients. (Recall that the cepstrum is normalized by twice the Nyquist frequency.) Again, since this is a numerically "clean" example, editing of this signal is fairly straightforward. Twenty-two of the highest level spikes in the cepstrum of figure 4(c) were edited out. Figure 4(d) shows the resulting edited free-field power spectrum, a good reconstruction of the free-field spectrum (fig. 2(b)).

3. EFFECT OF ADDITIVE NOISE

Theory

An important case occurs when noise is present in addition to the direct and reflected signals. The model for this is

$$x(t) = g(t) + \alpha g(t - t_e) + n(t)$$

The Fourier transform is

$$X(f) = \left(1 + \alpha\, e^{-i2\pi f t_e}\right) G(f) + N(f)$$

The power spectrum may be expressed as

$$|X(f)|^2 = X(f)X^*(f)$$

$$= \left[1 + \frac{2\alpha}{1 + \alpha^2} \cos(2\pi f t_e)\right](1 + \alpha^2)\ |G(f)|^2$$

$$+ |N(f)|^2 + 2\{[1 + \alpha \cos(2\pi f t_e)][G_r(f)N_r(f) + G_i(f)N_i(f)]$$

$$- \alpha \sin(2\pi f t_e)[G_r(f)N_i(f) - G_i(f)N_r(f)]\} \qquad (21)$$

where G_r, N_r, G_i, and N_i are the real and imaginary parts of $G(f)$ and $N(f)$. The first term is identical to that of equation (6), and the last three terms are due to the noise. If $N(f)$ is small compared with $G(f)$, the contribution of the noise terms may be negligible, but if $N(f)$ is large enough, these terms will contaminate the power spectrum and the power cepstrum. The contamination consists of the noise power spectrum $|N(f)|^2$ and the "cross terms" (i.e., $G_r(f)N_r(f)$, $G_i(f)N_i(f)$, $G_r(f)N_i(f)$, and $G_i(f)N_r(f)$).

A probabilistic study (refs. 22 and 23) has concluded that the effect of the cross terms is to lower and broaden the cepstrum echo peaks. The degree of contamination is related to both the frequency dependence of the signal-to-noise ratio and the relative bandwidths of the signal and noise (refs. 22 to 24). There are several approaches which can be used to avoid or decrease this noise contamination. If $n(t)$ could be measured without the source signal present, it could be subtracted from $x(t)$. Similarly, if $N(f)$ is known, it could be removed from $X(f)$ or $|X(f)|^2$. Ensemble averaging in the time domain would also serve to remove some of the noise content, but such time averaging would also remove any random content of $x(t)$, which may or may not be desirable. Averaging of the Fourier transforms would yield essentially the same results as averaging in the time domain. Averaging of the power spectra would eliminate the noise cross terms, since the signal and noise functions are incoherent. However, averaging of the power spectra will not remove the

noise power spectrum $|N(f)|^2$. Averaging in the cepstral domain has also been suggested (ref. 15). Such averaging procedures and data manipulation must be carefully chosen based on the character of the data (i.e., random, coherent, or both).

Numerical Examples

To qualitatively investigate the effect of additive noise, a composite signal consisting of the exponential impulse and echo of figure 3 with an additive random "background" noise function

$$x(t) = e^{-k|t-t_1|} + \alpha e^{-k|t-t_2|} + n(t)$$

was constructed to simulate the power spectrum described by equation (21). (See fig. 5.) The noise function $n(t)$ was obtained from a software random number generator. The signal-to-noise ratio of the exponential signal and echo to the noise is about 20 dB. The amplitude of the cepstrum spike at $\tau = 0.0018$ sec is significantly less than expected for an echo of $\alpha = 0.5$, and rahmonics are not present because of the noise, as shown in figure 5(c). The cepstrum spike amplitude is approximately 0.10, as opposed to an amplitude of 0.50 shown in figure 3(c) for the "clean" transient signal. Removal of this single spike results in a partial improvement in the echo ripple in the power spectrum. (Compare fig. 5(d) with the corrected spectrum without noise, fig. 3(d).) This illustrates that the additional noise terms of equation (21) can contaminate the cepstrum sufficiently to destroy the effectiveness of the approach, even if the noise $N(f)$ is small compared with the desired signal and echo. This example can be considered a "worst case" for two reasons: (1) no noise-removal approach, such as temporal, spectral, or cepstral averaging, is attempted; and (2) the relative signal-to-noise ratio of the exponential signal to the noise is quite small over most of the spectrum above a frequency of 10 kHz.

To verify the results of references 22 to 24 (i.e., that the noise contamination is related to the frequency variation of the signal-to-noise ratio and to the relative bandwidths of the signal and noise), two other cases were investigated. The first was the case of increasing the signal-to-noise ratio over that of figure 5; the second was the case of increasing the signal-to-noise ratio and widening the signal bandwidth relative to the noise bandwidth.

Figure 6 illustrates the effect of increasing the signal-to-noise ratio of the previous example from 20 to 32 dB. The cepstrum shown in figure 6(c) is very similar to that of the previous case, except that the spike amplitude has increased by a factor of two to a value of 0.22. This is closer to the desired value of 0.50 which would result if no noise were present. If we edit the cepstrum and perform the inverse Fourier transform, the corrected spectrum of figure 6(d) is found. This is a better estimate of the free-field spectrum than figure 5(d), although a small echo ripple remains.

Figure 7 illustrates the case of a larger signal bandwidth relative to the noise bandwidth. In this example the exponential factor k was increased from 6000 to 20 000, providing a broader signal spectrum. The normalized cepstrum (fig. 7(c)) exhibits a prominent echo spike at the correct delay time, with an amplitude approaching the desired level of 0.50. The first echo spike and one rahmonic were edited and the reconstructed spectrum is shown in figure 7(d).

4. EFFECT OF ECHO DISTORTION

Theory

The case of a direct signal and a distorted echo is also of great practical importance and can be modeled as

$$x(t) = g(t) + h(t - t_e)*g(t)$$

where the asterisk denotes a convolution and $h(t)$ is the impulse response function of the echo process. The Fourier transform and power spectrum may be written as

$$X(f) = \left[1 + H(f)\, e^{-2\pi f t_e}\right] G(f)$$

$$|X(f)|^2 = \left[1 + H(f)\, e^{-i2\pi f t_e}\right]\left[1 + H^*(f)\, e^{i2\pi f t_e}\right] |G(f)|^2 \qquad (22)$$

If we take the logarithm and use a power series expansion, the log power spectrum is

$$\ln|X(f)|^2 = \ln|G(f)|^2 + H(f)\, e^{-i2\pi f t_e} + H^*(f)\, e^{i2\pi f t_e}$$

$$- \tfrac{1}{2}\left[H(f)\right]^2 e^{-i4\pi f t_e} - \tfrac{1}{2}\left[H^*(f)\right]^2 e^{i4\pi f t_e} + \cdots$$

and the power cepstrum is

$$C_p(\tau) = C_{pg}(\tau) + \int_{-f_N}^{f_N} H(f)\, e^{i2\pi f(\tau - t_e)}\, df + \int_{-f_N}^{f_N} H^*(f)\, e^{i2\pi f(\tau + t_e)}\, df$$

$$- \frac{1}{2}\int_{-f_N}^{f_N} \left[H(f)\right]^2 e^{i2\pi f(\tau - 2t_e)}\, df - \frac{1}{2}\int_{-f_N}^{f_N} \left[H^*(f)\right]^2 e^{i2\pi f(\tau + 2t_e)}\, df + \cdots$$

$$= C_{pg}(\tau) + h(\tau - t_e) + h(\tau + t_e) - \tfrac{1}{2}\left[h(\tau - 2t_e) * h(\tau - 2t_e)\right]$$

$$- \tfrac{1}{2}\left[h(\tau + 2t_e) * h(\tau + 2t_e)\right] + \cdots$$

where $H(f)$ is the transfer function of the echo process and the superscript asterisk denotes the complex conjugate. Note that if $H(f)$ is a constant, causing a perfect echo, then $h(\tau - t_e)$ reduces to the $\frac{\sin[(nt_e - \tau)2\pi f_N]}{(nt_e - \tau)2\pi f_N}$ term of equation (11).

This case has been studied in detail by Hassab and Boucher (refs. 22 and 23) and by Bolton and Gold (ref. 15). The conclusions of reference 22 show that with distortion, the cepstrum echo spikes are lowered and broadened, qualitatively a similar effect as was shown in the presence of additive noise. This effect on the cepstrum spikes depends on the transfer function $H(f)$ of the echo process, which of course is generally unknown. The echo process can be considered as the sum of the reflector's transfer function and the acoustic propagation path.

The echo information in the cepstral domain is now "windowed," or smeared, by the transfer function in the same manner that windowing in the frequency domain occurs. The echo no longer appears as a discrete spike at the echo delay time and editing the cepstrum to remove the echo becomes substantially less straightforward.

Correction of Echo Transfer Function

To remove the contamination in the power spectrum due to the distorted echo, another approach is suggested. This approach requires an accurate knowledge of the transfer function of the echo process and an accurate knowledge of the echo delay time t_e. The complex impedance of the reflector and the acoustic propagation effects can be obtained through the use of standard techniques. The complex impedance can also be found with the cepstrum technique of reference 15. An accurate estimate of the echo delay time can be obtained easily from the power cepstrum of the contaminated signal. Now equation (22) may be rewritten as

$$|X(f)|^2 = \left[1 + 2H_r(f)\cos(2\pi f t_e) + 2H_i(f)\sin(2\pi f t_e) + |H(f)|^2\right]|G(f)|^2 \qquad (23)$$

Rearranging these terms, we can find the desired free-field power spectrum $|G(f)|^2$ by correcting the contaminated power spectrum $|X(f)|^2$ as follows:

$$|G(f)|^2 = \frac{|X(f)|^2}{1 + 2H_r(f)\cos(2\pi f t_e) + 2H_i(f)\sin(2\pi f t_e) + |H(f)|^2} \qquad (24)$$

The advantages of this technique are that the case-by-case editing of the cepstrum and the inverse transform processes are not required and that a routine correction to all measured power spectra can be employed. Elimination of the cepstrum editing and the inverse transform processes will be particularly beneficial when the cepstrum is difficult to edit due to noise or periodic content. The disadvantage to this technique is that it requires a knowledge of the echo transfer function $H(f)$.

Example of Transfer-Function Correction

To verify the validity of this transfer-function correction procedure, the procedure was applied to measured acoustic impulse data containing an echo. The impulse data were obtained during a model helicopter-rotor wind tunnel test in the Langley 4- by 7-Meter Tunnel in which remotely ignited blasting caps were mounted in the center of the tunnel test section. The direct blast signal and echoes were measured at all the microphone locations in the test section. Since the direct and echoed signals of the impulse occupy different regions of the acoustic time series, the Fourier transform of each impulse ($X_d(f)$ and $X_e(f)$) may be calculated separately, and then the echo transfer function may be estimated.

Equation (22) may be expressed as the sum of the Fourier transforms of the direct signal ($X_d(f)$) and the echoed signal ($X_e(f)$) as follows:

$$X(f) = \left[1 + H(f)\, e^{-i2\pi f t_e}\right] G(f) = X_d(f) + X_e(f)$$

where

$$X_d(f) = G(f)$$

and

$$X_e(f) = H(f)\, e^{-i2\pi f t_e}\, G(f)$$

The ratio of $X_d(f)$ and $X_e(f)$ are used to define a function $R(f)$:

$$R(f) = \frac{X_e(f)}{X_d(f)} \tag{25}$$

With $R(f)$, $H(f)$ may be found from

$$H(f) = e^{i2\pi f t_e}\, R(f)$$

From equation (24) with $H(f)$ and t_e, the free-field spectrum may be found.

Figure 8(a) presents the impulsive acoustic signal with a relatively strong reflection (echo) measured with a microphone very close to the tunnel test section floor. The regions marked in the figure indicate the data which were used to independently calculate the Fourier transforms of the direct and echoed signals. The same record length was used for each, with all nonpertinent data points before or

after the transient impulses set to zero. Figures 8(b) and 8(c) show the power spectra of the direct and echoed signals. These data were then used to calculate $R(f)$ from equation (25). Figure 8(d) shows the power spectrum of the direct plus the echoed signal. The objective is to correct this contaminated spectrum for the nonlinear echo and to reconstruct the uncontaminated spectrum of the direct wave (fig. 8(b)).

To calculate the function $H(f)$, an estimate of the echo time delay t_e is required. This value is estimated to be 0.003 sec from the power cepstrum of the contaminated spectrum (shown in fig. 9(a)). The transfer function $H(f)$ may now be found from $R(f)$ and t_e. The power spectrum $|H(f)|^2$ is shown in figure 9(b). When the contaminated spectrum is corrected for $H(f)$ as defined by equation (24), the spectrum shown in figure 9(c) is found. This spectrum compares very well with that of the direct wave presented in figure 8(b).

It is interesting to compare this correction procedure with the process of editing the cepstrum. The cepstrum shown in figure 9(a) was edited by setting all values greater than $\tau = 0.002$ sec to zero. The resulting spectrum is shown in figure 9(d). (Such severe cepstrum editing is valid when the time signal is transient or nonperiodic, since the cepstrum of the direct signal is small for large values of τ. The hump in the cepstrum near $\tau = 0.003$ sec (fig. 9(a)) is attributed to the windowing effect of the nonlinear transfer function acting on the echoed signal.) In a comparison of the two reconstructed spectra with the spectrum of the direct signal alone (fig. 8(b)), the spectrum corrected for the echo transfer function (fig. 9(c)) is clearly superior. The spectrum corrected with the cepstrum correction process (fig. 9(d)) yields a satisfactory result only at frequencies less than 2 kHz.

While performing these calculations, we noticed that the transfer functions calculated were extremely sensitive to the specific data used in each transform, the sample length, the sample rate, the transform size, and other particulars of the analysis. Although the spectral shapes were generally the same, the amplitudes would vary widely with small differences in the analysis approach. We feel that this was due to the paucity of data available to estimate the transfer function. Other approaches to finding the echo transfer function may prove more successful than that employed in this work.

5. APPLICATION TO PERIODIC FUNCTIONS

Much previous work on the topic of cepstrum echo removal has concluded that the technique is most successful if applied to cepstra which decay rapidly with quefrency τ. Typically these cepstra are for random or noncoherent functions. Deterministic or periodic functions, which are coherent, generally exhibit periodic characteristics in their cepstra. (Recall that the autocorrelation of a sinusoid is sinusoidal.) In preparation for the application of the cepstrum echo removal technique to measured helicopter-rotor acoustic data (which is considered highly tonal noise), the application of the technique to a generalized periodic function was investigated. The example periodic function considered is a set of harmonic sine waves of equal amplitude. Several examples are considered which have different contributions (i.e., source-related, non-source-related, and leakage-related contributions) at the off-harmonic frequencies.

Numerical Examples

Direct signal.- Figure 10(a) presents the power spectrum of the example periodic function, a series of 25 equal-amplitude harmonics of a fundamental 5-Hz tone with no echo contamination. The source signal has a constant off-harmonic level of about 76 dB. Figure 10(b) presents the normalized power cepstrum of this signal. Note the strong periodic character of the cepstrum. The spikes at $\tau = 0.20$ (t_f) and $\tau = 0.40$ are due to the fundamental tone frequency of 5 Hz. The oscillatory periodicity of the cepstrum is due to the harmonics present.

One ideal reflection ($t_e = 0.07$ sec).- Figure 11(a) presents the power spectrum of the same signal as used for figure 10 with the addition of an echo ($\alpha = 0.5$) at a delay time of 0.07 sec. The cepstrum (fig. 11(b)) clearly identifies this echo at $\tau = 0.07$ sec (t_e), and one rahmonic is evident at $\tau = 0.14$ sec $(2t_e)$. Note that the magnitude of the echo spike at $\tau = 0.07$ sec is very close to the expected level of 0.50 ($\alpha = 0.5$). Editing and interpolating of this type of cepstrum is not straightforward because of its harmonic character. Figure 11(c) presents the edited power cepstrum, and figure 11(d) presents the reconstructed power spectrum. A substantial part (though not all) of the echo ripple has been removed.

One ideal reflection ($t_e = 0.07$ sec) with leakage.- Another case of interest is that of the series of harmonic tones with no off-harmonic spectral content except that caused by numerical leakage or by the spectral leakage associated with use of a sample period which is not exactly an integer multiple of the fundamental period. Figure 12(a) presents the case of the same series of tones and an echo ($\alpha = 0.5$ and $t_e = 0.07$ sec) as used for figure 11(a) with no other source-related energy in the off-harmonic bands. The leakage energy is apparent in between the harmonic tones at a level of about 10 dB. The power cepstrum (fig. 12(b)) contains an echo spike at the correct delay time, although the spike amplitude is somewhat lower (0.40) than the expected value of 0.50. This lowering of the echo-spike level is attributed to the lack of significant energy in the off-harmonic bands to carry the echo ripple information.

One ideal reflection ($t_e = 0.29$ sec).- Figure 13 shows the same periodic function presented in figure 12 with an echo of $\alpha = 0.5$ at $t_e = 0.29$ sec. The power cepstrum (fig. 13(b)) of this signal exhibits an echo spike at $\tau = 0.09$ sec. In this case the echo ripple in the power spectrum has effectively been undersampled, and the information has been aliased in very much the same manner as aliasing in the frequency domain can occur. Instead of identifying an echo at $\tau = t_e$ (i.e., at 0.29 sec), the process has identified an echo at $\tau = t_e - t_f$ (0.29 - 0.20 = 0.09 sec), an aliased time delay. (Recall that t_f is the period of the 5-Hz tone.) This misidentification is attributed to the following: because there is not significant source-related energy in the off-harmonic bands to represent the echo ripple in the spectrum, the harmonic tone frequency becomes the "effective sample rate" of the spectrum; and because the harmonic tone frequency (sample rate) of 5 Hz is greater than the echo ripple frequency ($1/t_e \approx 3.5$ Hz), aliasing occurs. This phenomenon is analogous to the sampling theorem for time series, which states that to resolve frequencies with a period of T, one must use a sample interval of less than T/2. Thus, to resolve a frequency of 3.5 Hz in the spectrum, the effective sample rate should be less than 1.7 Hz.

One ideal reflection ($t_e = 0.07$ sec) with additive noise.- A final example (figs. 14 and 15) involves the same periodic function as that used for figures 11 to 13 with an off-harmonic level which is unrelated to the source signal; this results

in an additive ambient noise level. This example, with an echo at $t_e = 0.07$ sec, is presented in figure 14(a). The cepstrum (fig. 14(b)) only weakly exhibits the echo spike. The same source signal with an echo at $t_e = 0.29$ sec is presented in figure 15(a). Again the cepstrum echo spike is very weak compared with the previous cases, and the echo time delay has been aliased from its actual value.

Discussion

The general conclusion from these results is that the measured source spectrum must be a continuous spectrum, that is, the spectral energy must all be due to the source signal and its echoes. If there are regions of the measured spectrum which are due to an extraneous source, then the echo ripple information will not be represented at these bands and the detection of the echo will be severely deteriorated. Although the numerical examples may seem purely academic, the situations modeled can easily occur in experimental measurements. Consider, for example, the measurement of a source with an echo when the source has a highly tonal or periodic content. The source may also have broadband content at the nontonal frequencies. If the off-harmonic source energy is significantly lower than the tone energy, it may be hidden by instrumentation noise during the data acquisition process. Thus, one could be faced with data very similar to that presented in figure 14, a periodic direct signal with an echo at harmonic frequencies, and a non-source-related off-harmonic "noise floor" which would not represent the echo ripple.

Other conclusions related to the application of the cepstrum to periodic data are as follows. The editing and interpolating procedure can be quite difficult, with potentially erratic results. For such signals, the correction technique presented in section 4 may be more useful. Clearly, the dynamic ranges of the data and of the data acquisition process are of importance, as is the origin of the spectral content (source- or non-source-related contribution). In addition, the ratio of the analysis bandwidth (1/T) to the echo ripple frequency ($1/t_e$) is important. In analogy to Shannon's sampling theorem, it is concluded that the analysis bandwidth should be less than one-half of the echo ripple frequency $1/t_e$, to prevent aliasing of the echo time delay in the cepstral domain. This is a similar conclusion to that previously reported (ref. 15), that the echo delay time should be less than one-half of the sample record length.

6. APPLICATION TO HELICOPTER-ROTOR ACOUSTIC DATA

The cepstrum correction technique was applied to measured model helicopter-rotor acoustic data containing reflections from a wind tunnel wall. These data were acquired in the Langley 4- by 7-Meter Tunnel. Acoustic results are reported in references 20 and 21. A diagnostic test was also performed to assess the magnitude of possible reflections from an impulsive point source at each microphone and to identify an approximate echo arrival time at each microphone. Estimates of the relative amplitudes were made from the acoustic time histories of these events, and estimates of the delay times were made from the power cepstra.

Helicopter-Rotor Noise Model

It should be recognized that helicopter-rotor noise consists of two general contributions. The highest noise levels are generated at a series of low-frequency harmonics of the blade-passage frequency f_{BP} (equal to the number of rotor blades

times the shaft rotation frequency; typically, f_{BP} = 15 to 20 Hz). This acoustic signal is highly periodic and discrete. The other major source is helicopter-rotor broadband noise (ref. 25), and although this source has some energy at the lower frequencies (those less than 1 kHz), most of the energy is in the middle frequency range (i.e., 1 to 5 kHz). This contribution is a more random and broadband noise source. Thus, the helicopter-rotor noise signal can be modeled as follows:

$$x(t) = \sum_{n=1}^{N} a(nf_{BP}) \sin(2\pi nf_{BP}t) + r(t) + n(t)$$

where $a(nf_{BP})$ is the amplitude envelope of the helicopter-rotor harmonics, N is the number of rotor harmonics, r(t) is the rotor broadband noise signal, and n(t) is the additive wind tunnel background noise. The rotor signal with one perfect reflection can be modeled as

$$x(t) = \sum_{n=1}^{N} a(nf_{BP})\left\{\sin(2\pi nf_{BP}t) + \alpha \sin\left[2\pi nf_{BP}(t - t_e)\right]\right\}$$

$$+ r(t) + \alpha r(t - t_e) + n(t)$$

Application

Power-averaged spectra.- The cepstrum technique was applied to the rotor acoustic data measured at a microphone located in the tunnel flow for a typical rotor test condition (i.e., 60 knots, 2° rotor angle of attack, microphone 3, and f_{BP} = 100 Hz). Since this was a 1/5-scale rotor model, the rotational speed was increased by five, causing the f_{BP} value of 100 Hz. Fifty power spectra of the rotor signal were averaged to obtain a power-averaged spectrum as follows:

$$\left|X(f)\right|^2_{avg} = \frac{1}{50} \sum_{i=1}^{50} \left|X_i(f)\right|^2$$

This is the conventional method of spectral averaging, as it preserves all the acoustic energy in the signal and does not remove random content. Another result of this spectral averaging process is to eliminate some of the cross term contributions of equation (21) as discussed in section 3. Note the ripple in the spectrum (fig. 16(a)), particularly obvious between 2000 and 6000 Hz. The period of this ripple is approximately 500 Hz, which corresponds to an echo time delay of 0.0020 sec. From the impulse data results, which are presented in table III of reference 20, we anticipate reflections occurring at echo delay times of approximately 0.0025 and 0.0240 sec with relative amplitudes of 0.49 and 0.10. The cepstrum is shown in figure 16(b), with two prominent spikes near 0.0020 and 0.0200 sec. (In these plots the first few points near zero have been set to zero to increase the plot resolution.) The rahmonics of these two spikes are not obvious. Note that except for the echo

spikes, the cepstrum shows a somewhat repeatable pattern. This pattern repeats every 0.01 sec, which is the period of the blade-passage frequency (100 Hz). The cepstrum echo spike at $\tau = 0.002$ sec corresponds to $\alpha \approx 0.18$, and the echo spike at $\tau = 0.020$ sec corresponds to $\alpha \approx 0.13$; these values of α are considerably different from the expected echo strengths (i.e., 0.49 and 0.10). This discrepancy in the data is partly due to the presence of background noise, which we have seen can lower the levels of the cepstrum echo peaks. It is also partly because the reflections are not perfect duplicates of the direct signals, another effect which tends to lower and broaden the echo spikes.

Some engineering judgment is required to remove the echo spikes since the cepstrum levels due to the direct signal at these values of τ are not known. The edited cepstrum is shown in figure 16(c), and the reconstructed spectrum is shown in figure 16(d). The harmonic ripple is almost completely removed from the measured spectrum except at the higher frequencies. The difference between the measured (contaminated) spectrum and the corrected spectrum is shown in figure 16(e). Although the difference in overall levels is 1.0 dB, the correction to individual frequency levels oscillates approximately ±4.0 dB.

Another example of data for a typical rotor-test condition (i.e., 55 knots, 6° rotor angle of attack, and microphone 2, $f_{BP} = 100$ Hz) is given in figure 17 for another inflow location. The ripple in the spectrum has a period of about 400 Hz (for an echo time delay of 0.0025 sec). From the impulsive data results (table III of ref. 20), we expect reflections at $\tau = 0.0031$ and 0.0098 sec. A large spike is shown in the cepstrum (fig. 17(b)) at $\tau = 0.0026$ sec. A spike at $\tau = 0.0090$ sec is also shown, but its amplitude is much less than the one at $\tau = 0.0026$ sec. This spike at $\tau = 0.0090$ sec could also be part of the natural periodicity of the cepstrum. If we had no prior knowledge of the possible echoes, this second reflection could easily be overlooked in the cepstrum. Thus, some knowledge of the probable echo delay time is desirable for the success of this technique. Note again the somewhat periodic character of the cepstrum. The effect of removing the first echo is shown in figures 17(c) and 17(d), which show the edited cepstrum and the reconstructed spectrum. Again, the ripple at the higher frequencies has been virtually removed. Although the correction to the overall sound level is 0.1 dB, the spectral differences are ±0.6 dB. (See fig. 17(e).)

Coefficient-averaged spectra.- To investigate the deterministic content of the data, a second method of spectral averaging was used. In this case, the Fourier coefficients of 50 spectra rather than the power of 50 spectra, are averaged as follows:

$$|X(f)|^2_{avg} = \left| \frac{1}{50} \sum_{i=1}^{50} X_i(f) \right|^2$$

This coefficient-averaging approach serves to average out random contributions to the signal, such as the helicopter-rotor broadband noise $r(t)$ and the tunnel background noise contamination $n(t)$. The same data of figure 16 were averaged in this manner and are presented in figure 18. For the comparison of the two methods of averaging, the overall sound level from the power-averaging method is 112.6 dB, whereas the overall sound level from the coefficient-averaging method is 107.2 dB. The blade-passage frequency, at approximately 100 Hz, has the same sound level for either averaging method. This indicates that it is primarily a pure harmonic signal with little

random content. (Recall that this was already suspected based on the 0.01-sec periodicity in the cepstrum of fig. 16(b).) Between 500 and 2500 Hz, the power-averaged levels are consistently larger than the coefficient-averaged levels, typically by 5 to 10 dB. Above 2500 Hz, the power-averaged levels are consistently 15 to 20 dB larger than the coefficient-averaged levels. This indicates that except at the fundamental frequency, the rotor signal contains a larger contribution from random sources than from deterministic sources or phenomena, although the character of the signal is quite discrete or tonal.

Discussion

A comparison of the cepstra obtained from the two averaging methods is interesting. (See figs. 16(b) and 18(b).) The cepstrum from the coefficient-averaged spectrum (fig. 18(b)) is much "noisier" than the power-averaged cepstrum (fig. 16(b)) and displays many spikes. This is probably due to the more tonal nature of the coefficient-averaged spectrum. A prominent spike is again shown at $\tau = 0.002$ sec and a less prominent spike is shown at $\tau = 0.020$. Interestingly, the cepstrum peak amplitudes at these echo times are almost the same in the two cepstra, and this indicates that the two averaging methods retain the same echo characteristics.

The fact that the cepstrum echo spikes have the same sound level for both averaging methods indicates that the noise $N(f)$ present in the power-averaged spectrum does not have a measurable effect on the total cepstrum at the echo peak location. It appears that the factor which has lowered the cepstrum echo peaks from the expected sound levels is the nonlinearity of the reflection process. The conclusion that echo distortion effects are more important than additive noise effects was also reached from the use of the power cepstrum with hydroacoustic data containing echoes (ref. 3) and in a general study of the comparative effects of distortion and noise on the cepstrum (ref. 22). Ideally, the removal of any nonlinearity in the echo transfer function is desirable, as illustrated by the simple example in section 4. Additional work was performed in an attempt to estimate a transfer function to correct the measured rotor data; however, this work proved largely unsuccessful. The lack of success is attributed to two factors: (1) the rotor is a large (i.e., 2.8-m-diameter) distributed-noise source which could receive echoes from reflectors different from those used to calculate the applied $H(f)$, and (2) an accurate $H(f)$ is difficult to calculate from the amount and type of available data from this experiment. In spite of these problems, it is still concluded that editing of the power cepstrum provides an improved estimate of the rotor free-field spectrum.

7. CONCLUSIONS

The application of the power cepstrum to remove acoustic reflections from measured helicopter-rotor acoustic spectra has been investigated. It was found that a previously applied correction to the reconstructed spectrum, which would require prior knowledge of the echo amplitude or path length, is not required or correct. Although information of the echo amplitude and delay time is helpful in applying this technique, the technique can often be applied with no prior information of the echo characteristics. It was also found that for the case of an exact echoed signal, the amplitude of the cepstrum echo spike at the echo delay time is linearly related to the relative amplitude of the echo in the time domain. It was found that for the best application of the technique, the entire measured spectrum must be from the source signal. If part of the source signal is masked by any extraneous non-source-related signal, the echo ripple in the power spectrum is not well represented. In

this case the cepstrum does not yield the desired echo characteristics and aliasing in the cepstral domain can occur because of the altered effective sample rate in the frequency domain. It was also found that to prevent aliasing of the echo delay time in the cepstral domain, the spectral analysis bandwidth (the inverse of the time series record) must be less than one-half of the echo ripple frequency (the inverse of the echo delay time).

The power cepstrum was found to be useful for removing some of the contamination from acoustic reflections in measured helicopter-rotor acoustic spectra. The cepstrum editing process was limited by the nonlinear transfer function acting on the acoustic reflections. Although cepstrum editing yielded an improved estimate of the free-field spectrum, there still remained some error because of the nonlinear transfer function of the echo process. An alternate procedure was proposed which would allow the complete correction of a contaminated spectrum by use of both the echo transfer function and the echo delay time. Although this procedure would remove the need for editing in the cepstral domain, it requires a knowledge of the transfer function of the echo process.

NASA Langley Research Center
Hampton, VA 23665-5225
March 10, 1986

APPENDIX A

AMPLITUDE OF ECHO CEPSTRUM AT $\tau = 0$

The derivation in this appendix is intended to prove that

$$\ln(1 + \alpha^2) - a_0 \equiv 0$$

A more complete expression of equation (10), the power cepstrum of $g(t)$ with one ideal echo, is helpful to this derivation and is given as follows:

$$C_p(\tau) = \int_{-f_N}^{f_N} \ln\left(|G(f)|^2\right) e^{i2\pi f\tau}\, df + \int_{-f_N}^{f_N} \ln(1 + \alpha^2)\, e^{i2\pi f\tau}\, df$$

$$+ \phi \int_{-f_N}^{f_N} \cos(2\pi f t_e)\, e^{i2\pi f\tau}\, df - \frac{1}{2}\phi^2 \int_{-f_N}^{f_N} \frac{1}{2}\left[1 + \cos(4\pi f t_e)\right] e^{i2\pi f\tau}\, df$$

$$+ \frac{1}{3}\phi^3 \int_{-f_N}^{f_N} \frac{1}{4}\left[3\cos(2\pi f t_e) + \cos(6\pi f t_e)\right] e^{i2\pi f\tau}\, df$$

$$- \frac{1}{4}\phi^4 \int_{-f_N}^{f_N} \frac{1}{8}\left[3 + 4\cos(4\pi f t_e) + \cos(8\pi f t_e)\right] e^{i2\pi f\tau}\, df$$

$$+ \frac{1}{5}\phi^5 \int_{-f_N}^{f_N} \frac{1}{16}\left[10\cos(2\pi f t_e) + 5\cos(6\pi f t_e) + \cos(10\pi f t_e)\right] e^{i2\pi f\tau}\, df$$

$$- \frac{1}{6}\phi^6 \int_{-f_N}^{f_N} \frac{1}{32}\left[10 + 15\cos(4\pi f t_e) + 6\cos(8\pi f t_e) + \cos(12\pi f t_e)\right] e^{i2\pi f\tau}\, df$$

$$+ \frac{1}{7}\phi^7 \int_{-f_N}^{f_N} \frac{1}{64}\left[35\cos(2\pi f t_e) + 21\cos(6\pi f t_e) + \ldots\right] e^{i2\pi f\tau}\, df$$

(Equation continued on the next page)

$$- \frac{1}{8}\phi^8 \int_{-f_N}^{f_N} \frac{1}{128}[35 + 56\cos(4\pi f t_e) + 28\cos(8\pi f t_e) + \ldots]\, e^{i2\pi f\tau}\, df$$

$$+ \frac{1}{9}\phi^9 \int_{-f_N}^{f_N} \frac{1}{256}[126\cos(2\pi f t_e) + 84\cos(6\pi f t_e) + \ldots]\, e^{i2\pi f\tau}\, df$$

$$- \frac{1}{10}\phi^{10} \int_{-f_N}^{f_N} \frac{1}{512}[126 + 210\cos(4\pi f t_e) + 120\cos(8\pi f t_e) + \ldots]\, e^{i2\pi f\tau}\, df$$

$$+ \ldots \qquad \text{(A1)}$$

This expression may be reduced to

$$C_p(\tau) = C_{pg}(\tau) + 2f_N[\ln(1 + \alpha^2) - a_0]\left[\frac{\sin(2\pi f_N \tau)}{2\pi f_N \tau}\right]$$

$$+ f_N \sum_{n=1}^{\infty} a_n \left\{ \frac{\sin[(nt_e - \tau)2\pi f_N]}{(nt_e - \tau)2\pi f_N} + \frac{\sin[(nt_e + \tau)2\pi f_N]}{(nt_e + \tau)2\pi f_N} \right\}$$

The form of the coefficient a_0 may be shown to be the series of factors multiplying all the integrals of $e^{i2\pi f\tau}$ in equation (A1). Thus, a_0 may be written as

$$a_0 = \frac{1}{2}\frac{1}{2}\phi^2 + \frac{1}{4}\frac{3}{8}\phi^4 + \frac{1}{6}\frac{10}{32}\phi^6 + \frac{1}{8}\frac{35}{128}\phi^8 + \frac{1}{10}\frac{126}{512}\phi^{10} + \ldots$$

$$= \frac{1}{4}\phi^2 + \frac{3}{32}\phi^4 + \frac{5}{96}\phi^6 + \frac{35}{1024}\phi^8 + \frac{63}{2560}\phi^{10} + \ldots$$

The entire factor multiplying the $(\sin x)/x$ term at $\tau = 0$ is $\ln(1 + \alpha^2) - a_0$. To prove that

$$\ln(1 + \alpha^2) - a_0 = 0$$

it is established that $\ln(1 + \alpha^2)$ is equal to the same infinite series as the coefficient a_0. To show this we define the quantity $(1 + \alpha^2)$ as a function of ϕ using the simplifying expression

$$\phi = \frac{2\alpha}{1 + \alpha^2} \tag{A2}$$

which may be rewritten as

$$\phi\alpha^2 - 2\alpha + \phi = 0$$

This is a quadratic equation in α with roots

$$\alpha = \frac{2 \pm \sqrt{4 - 4\phi^2}}{2\phi} = \frac{1}{\phi} \pm \frac{1}{\phi}\sqrt{1 - \phi^2}$$

Now, since $0 \leq \alpha < 1.0$, we must take only the root

$$\alpha = \frac{1}{\phi} - \frac{1}{\phi}\sqrt{1 - \phi^2} \tag{A3}$$

From this relation and

$$\left(1 - \sqrt{1 - \phi^2}\right)\left(1 + \sqrt{1 - \phi^2}\right) = \phi^2$$

equation (A3) may be expressed in terms of ϕ as

$$\alpha = \frac{\phi}{1 + \sqrt{1 - \phi^2}} \tag{A4}$$

To find the quantity $1 + \alpha^2$ in terms of ϕ, equation (A2) is inverted and equation (A4) is used to define α:

$$1 + \alpha^2 = \frac{2\alpha}{\phi} = \frac{2}{1 + \sqrt{1 - \phi^2}}$$

Taking the natural logarithm and separating terms results in

$$\ln(1 + \alpha^2) = \ln\left(\frac{2}{1 + \sqrt{1 - \phi^2}}\right) = \ln 2 - \ln\left(1 + \sqrt{1 - \phi^2}\right) \tag{A5}$$

From reference 26, we find the useful identity

$$\ln\left(1 + \sqrt{1 + x^2}\right) = \ln 2 - \sum_{k=1}^{\infty} (-1)^k \frac{(2k - 1)!}{2^{2k}(k!)^2} x^{2k} \qquad (x^2 < 1)$$

Letting $x = i\phi$ to introduce a negative sign under the square root, we may write the identity as

$$\ln\left(1 + \sqrt{1 - \phi^2}\right) = \ln 2 - \sum_{k=1}^{\infty} (-1)^k \frac{(2k - 1)!}{2^{2k}(k!)^2} (i\phi)^{2k}$$

$$= \ln 2 - \sum_{k=1}^{\infty} \frac{(2k - 1)!}{2^{2k}(k!)^2} \phi^{2k} \tag{A6}$$

By substitution of equation (A6) into (A5),

$$\ln(1 + \alpha^2) = \ln 2 - \left[\ln 2 - \sum_{k=1}^{\infty} \frac{(2k - 1)!}{2^{2k}(k!)^2} \phi^{2k}\right] = \sum_{k=1}^{\infty} \frac{(2k - 1)!}{2^{2k}(k!)^2} \phi^{2k}$$

Since

$$\sum_{k=1}^{\infty} \frac{(2k - 1)!}{2^{2k}(k!)^2} \phi^{2k} = \frac{1}{4}\phi^2 + \frac{3}{32}\phi^4 + \frac{5}{96}\phi^6 + \frac{35}{1024}\phi^8 + \frac{63}{2560}\phi^{10} + \ldots = a_0$$

this shows that

$$\ln(1 + \alpha^2) - a_0 \equiv 0$$

Thus, there is no $(\sin x)/x$ term because of the echo in the power cepstrum at $\tau = 0$.

APPENDIX B

AMPLITUDE OF ECHO CEPSTRUM AT $\tau = t_e$

The derivation in this appendix is intended to prove equation (15):

$$a_1 = \sum_{j=1}^{\infty} \left(\frac{1}{2j - 1}\right) \frac{(2j - 1)!}{2^{2j-2}(j - 1)!j!} \phi^{2j-1} = 2\alpha$$

In this series, the first fraction $(1/(2j - 1))$ results from the logarithm expansion and the second fraction $((2j - 1)!/[2^{2j-2}(j - 1)!j!])$ results from the expansion for powers of the cosine function, as discussed in section 2.

For values of $\phi < 1.0$, the series for a_1 converges to the quantity 2α. To prove this, we start by rewriting 2α in terms of ϕ using equation (A3):

$$2\alpha = \frac{2}{\phi}\left(1 - \sqrt{1 - \phi^2}\right) \tag{B1}$$

The problem now is to prove that equation (B1) converges to equation (15):

$$\frac{2^2}{\phi} \sum_{j=1}^{\infty} \left(\frac{\phi}{2}\right)^{2j} \frac{(2j - 2)!}{(j - 1)!j!} = \frac{2}{\phi}\left(1 - \sqrt{1 - \phi^2}\right) \tag{B2}$$

The right side of equation (B2) may be rewritten as a series, with the binomial expansion for $\sqrt{1 - x^2}$, as

$$\left(1 - \sqrt{1 - \phi^2}\right) = \frac{1}{2}\phi^2 + \frac{1}{2}\frac{1}{4}\phi^4 + \frac{1}{2}\frac{1}{4}\frac{3}{6}\phi^6 + \frac{1}{2}\frac{1}{4}\frac{3}{6}\frac{5}{8}\phi^8 + \ldots \tag{B3}$$

With the following definitions,

$$(-1)!! = 1$$

$$(2j + 1)!! = 1 \cdot 3 \cdot 5 \ldots (2j + 1)$$

$$(2j)!! = 2 \cdot 4 \cdot 6 \ldots (2j)$$

equation (B3) may be rewritten in the condensed form as

$$\left(1 - \sqrt{1 - \phi^2}\right) = \sum_{j=1}^{\infty} \frac{(2j - 3)!!}{2j!!} \phi^{2j} \tag{B4}$$

By induction it can be shown that

$$2 \sum_{j=1}^{\infty} \left(\frac{\phi}{2}\right)^{2j} \frac{(2j - 2)!}{(j - 1)!n!} = \sum_{j=1}^{\infty} \frac{(2j - 3)!!}{(2j)!!} \phi^{2j}$$

or that

$$\frac{(2j - 2)!}{2^{2j-1}(j - 1)!j!} = \frac{(2j - 3)!!}{(2j)!!} \tag{B5}$$

as follows: Step 1 is to show that equation (B5) is true for $j = 1$:

$$\frac{[2(1) - 2]!}{2^{2(1)-1}(1 - 1)!1!} = \frac{[2(1) - 3]!!}{[2(1)]!!}$$

which results in

$$\frac{1}{2} = \frac{1}{2}$$

Step 2 is to assume equation (B5) is true for $j = k$ and to show it is true for $j = k + 1$.

$$\frac{[2(k + 1) - 2]!}{2^{2(k+1)-1}k!(k + 1)!} = \frac{[2(k + 1) - 3]!!}{[2(k + 1)]!!}$$

which reduces to

$$\frac{(2k)!}{2^{2k+1}k!(k + 1)!} = \frac{(2k - 1)(2k - 3)!!}{(2k + 2)(2k)!!}$$

With equation (B5), the above expression is rewritten as

$$\frac{2(k)!}{2^{2k+1}k!(k+1)!} = \frac{(2k-1)(2k-2)!}{(2k+2)2^{2k-1}(k-1)!k!}$$

which readily reduces to

$$\frac{2}{2^{2k}(2k+2)} = \frac{2}{2^{2k}(2k+2)}$$

Thus,

$$a_1 = \sum_{j=1}^{\infty} \frac{\phi^{2j-1}(2j-2)!}{2^{2j-2}(j-1)!j!} = \frac{2}{\phi}\left(1 - \sqrt{1-\phi^2}\right) = 2\alpha$$

REFERENCES

1. Bogert, Bruce P.; Healy, M. J. R.; and Tukey, John W.: The Quefrency Analysis of Time Series for Echoes: Cepstrum, Pseudo-Autocovariance, Cross-Cepstrum and Saphe Cracking. Time Series Analysis, Murray Rosenblatt, ed., John Wiley & Sons, Inc., pp. 209-243.

2. Cohen, T. J.: Source-Depth Determination Using Spectral, Pseudo-Autocorrelation and Cepstral Analysis. Geophys. J., vol. 20, no. 2, Aug. 1970, pp. 223-231.

3. Fjell, Per O.: Use of the Cepstrum Method for Arrival Times Extraction of Overlapping Signals Due to Multipath Conditions in Shallow Water. J. Acoust. Soc. America, vol. 59, no. 1, Jan. 1976, pp. 209-211.

4. Schafer, Ronald W.; and Rabiner, Lawrence R.: System for Automatic Formant Analysis of Voiced Speech. J. Appl. Syst. Anal., vol. 47, no. 2, pt. 2, Feb. 1970, pp. 634-648.

5. Oppenheim, Alan V.: Speech Analysis-Synthesis System Based on Homomorphic Filtering. J. Appl. Syst. Anal., vol. 45, no. 2, Feb. 1969, pp. 458-465.

6. Kemerait, R. C.; and Childers, D. G.: Signal Detection and Extraction by Cepstrum Techniques. IEEE Trans. Inf. Theory, vol. IT-18, no. 6, Nov. 1972, pp. 745-759.

7. Kemerait, R. C.; and Childers, D. G.: Detection of Multiple Echoes Immersed in Noise. Proceedings of the Fifteenth Midwest Symposium on Circuit Theory, Volume 1, Dep. Electr. Eng., Univ. of Missouri-Rolla, May 1972, pp. VI.4.1-VI.4.10.

8. Halpeny, Owen Simeon: Epoch Detection of Digital Cepstrum Analysis. M.S. Thesis, Univ. of Florida, 1970.

9. Randall, R. B.: Cepstrum Analysis and Gearbox Fault Diagnosis - Edition 2. Appl. Note 233-80, Bruel & Kjaer. (Replaces Appl. Note No. 13-150, 1973).

10. Syed, A. A.; Brown, J. D.; Oliver, M. J.; and Hills, S. A.: The Cepstrum: A Viable Method for the Removal of Ground Reflections. J. Sound & Vib., vol. 71, no. 2, July 22, 1980, pp. 299-313.

11. Miles, J. H.; Stevens, G. H.; and Leininger, G. G.: Analysis and Correction of Ground Reflection Effects in Measured Narrowband Sound Spectra Using Cepstral Techniques. NASA TM X-71810, [1975].

12. Miles, Jeffrey H.; Stevens, Grady H.; and Leininger, Gary G.: Application of Cepstral Techniques to Ground-Reflection Effects in Measured Acoustic Spectra. J. Acoust. Soc. America, vol. 61, no. 1, Jan. 1977, pp. 35-38.

13. Miles, J. H.; and Wasserbauer, C. A.: Analysis of Combustion Spectra Containing Organ Pipe Tones by Cepstral Techniques. NASA TM-83034, [1982].

14. Poché, Lynn B., Jr.: Complex Cepstrum Processing of Digitized Transient Calibration Data for Removal of Echoes. NRL Rep. 8143, U.S. Navy, Sept. 1977. (Available from DTIC as AD A047 414.)

15. Bolton, J. S.; and Gold, E.: The Application of Cepstral Techniques to the Measurement of Transfer Functions and Acoustical Reflection Coefficients. J. Sound & Vib., vol. 93, no. 2, Mar. 22, 1984, pp. 217-233.

16. Bright, K.; and Thomas, D. W.: Effect of Manifold Design and Firing Order on the Short Term Spectrum. J. Sound & Vib., vol. 48, no. 3, Oct. 8, 1976, pp. 393-403.

17. Childers, Donald G.; Skinner, David P.; and Kemerait, Robert C.: The Cepstrum: A Guide to Processing. IEEE Proc., vol. 65, no. 10, Oct. 1977, pp. 1428-1443.

18. Randall, R. B.; and Hee, Jens: Cepstrum Analysis. Tech. Rev., no. 3, Bruel & Kjaer Instruments, Inc., 1981, pp. 3-40.

19. Martin, R. M.; Elliott, J. W.; and Hoad, D. R.: Comparison of Experimental and Analytical Predictions of Rotor Blade-Vortex Interactions Using Model Scale Acoustic Data. AIAA-84-2269, Oct. 1984.

20. Martin, R. M.; and Connor, Andrew B.: Wind-Tunnel Acoustic Results of Two Rotor Models With Several Tip Designs. NASA TM-87698, 1986.

21. Hayden, R. E.; and Wilby, J. F.: Sources, Paths, and Concepts for Reduction of Noise in the Test Section of the NASA Langley 4 × 7m Wind Tunnel. NASA CR-172446-1, 1984.

22. Hassab, J. C.; and Boucher, R.: Analysis of Signal Extraction, Echo Detection and Removal by Complex Cepstrum in Presence of Distortion and Noise. J. Sound & Vib., vol. 40, no. 3, June 8, 1975, pp. 321-335.

23. Hassab, Joseph C.; and Boucher, Ronald: A Probabilistic Analysis of Time Delay Extraction by the Cepstrum in Stationary Gaussian Noise. IEEE Trans. Inf. Theory, vol. IT-22, no. 4, July 1976, pp. 444-454.

24. Balluet, J. C.; Lacoume, J. L.; and Baudois, D.: Séparation de Deux Échos Rapprochés par le Cepstre d'Énergie. Ann. Telecommun., vol. 36, no. 7-8, 1981, pp. 439-456.

25. Brooks, Thomas F.; and Schlinker, Robert H.: Progress in Rotor Broadband Noise Research. Vertica, vol. 7, no. 4, 1983, pp. 287-307.

26. Gradshteyn, I. S.; and Ryzhik, I. M. (Scripta Technica, Inc., transl.): Table of Integrals, Series, and Products, Fourth ed. Academic Press, Inc., c.1965.

SYMBOLS

a_n	coefficients of cepstrum echo peaks for one-echo case (n = 0, 1, 2, ...)
$a(nf_{BP})$	amplitude envelope of helicopter-rotor harmonic tones (nf_{BP})
C_p	power cepstrum, inverse Fourier transform of logarithm of power spectrum
C'_p	edited power cepstrum
C_{pg}	power cepstrum of g(t)
f	frequency, Hz
f_{BP}	blade-passage frequency of helicopter-rotor acoustic signal, equal to number of rotor blades times shaft rotation frequency, Hz
f_f	fundamental tone frequency, Hz
f_N	Nyquist frequency, Hz
G(f)	Fourier transform of direct signal g(t)
g(t)	general function of direct signal
H(f)	Fourier transform of transfer function of echo process
h(t)	impulse response function of echo process
i	imaginary part of complex conjugate
k	power of example exponential functions
N(f)	Fourier transform of noise function n(t)
n(t)	noise function
R(f)	ratio of $X_e(f)$ to $X_d(f)$
$R_x(\tau)$	autocorrelation function
r(t)	helicopter-rotor broadband noise signal
T	period of time series used in Fourier analysis, sec
t	time, sec
t_e	echo delay time of one-echo signal, sec
t_f	period of tone frequency, sec
t_1	echo delay time of first echo in two-echo signal, sec
t_2	echo delay time of second echo in two-echo signal, sec

$X(f)$ Fourier transform of $x(t)$

$X_d(f)$ Fourier transform of direct signal $x(t)$

$X_e(f)$ Fourier transform of echoed signal $x(t)$

$x(t)$ general function of time

α amplitude ratio of first echo to direct signal

β amplitude ratio of second echo to direct signal

τ quefrency, sec

ϕ $= \frac{2\alpha}{1 + \alpha^2}$

Subscripts:

avg averaged quantity

r real part of complex variable

A superscript asterisk * indicates a complex conjugate.

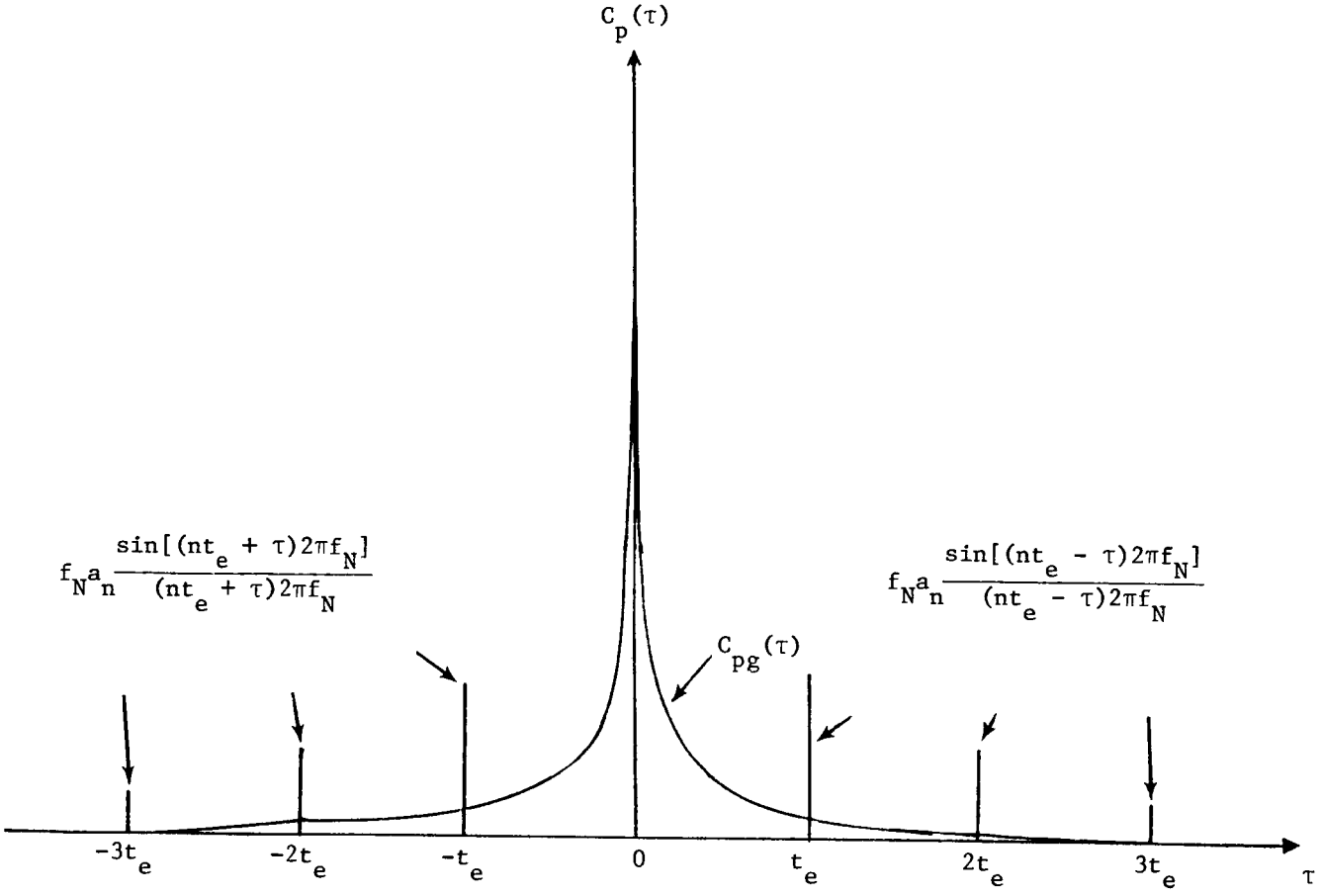

Figure 1.- Model of power cepstrum of general random signal with one ideal echo.

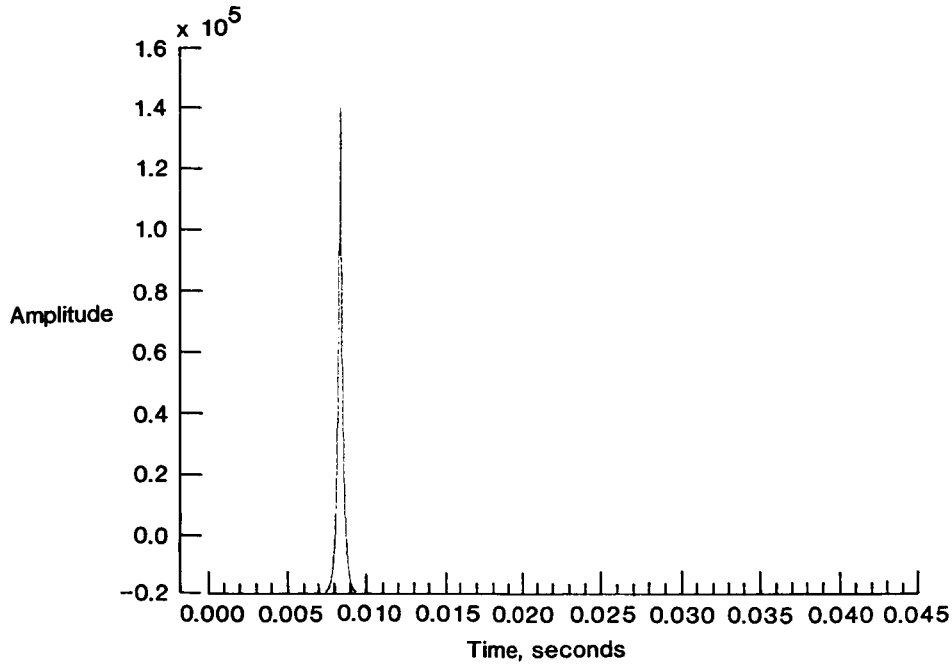

(a) Time history.

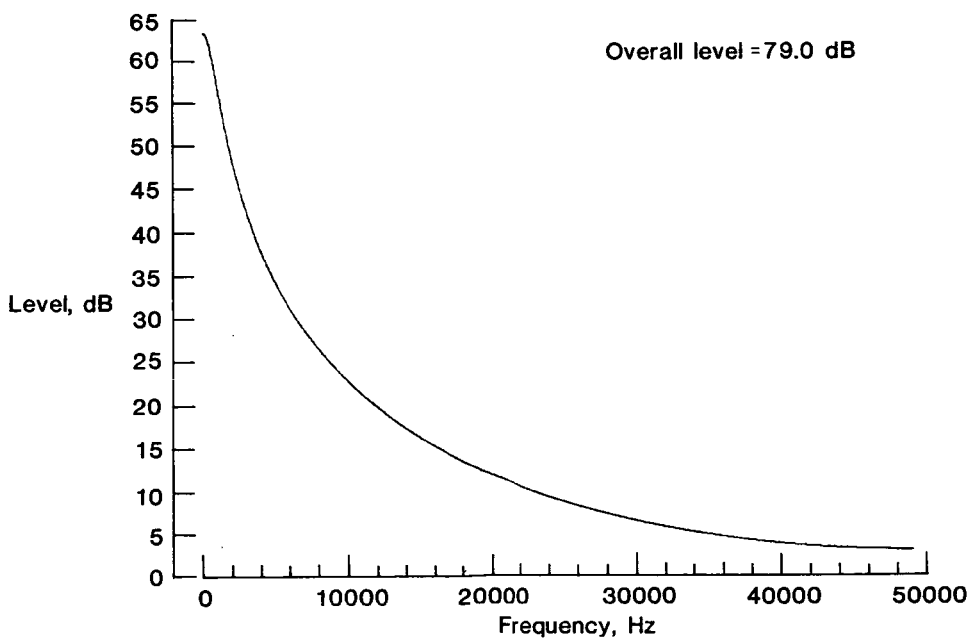

(b) Power spectrum.

Figure 2.- Exponential signal without echo.

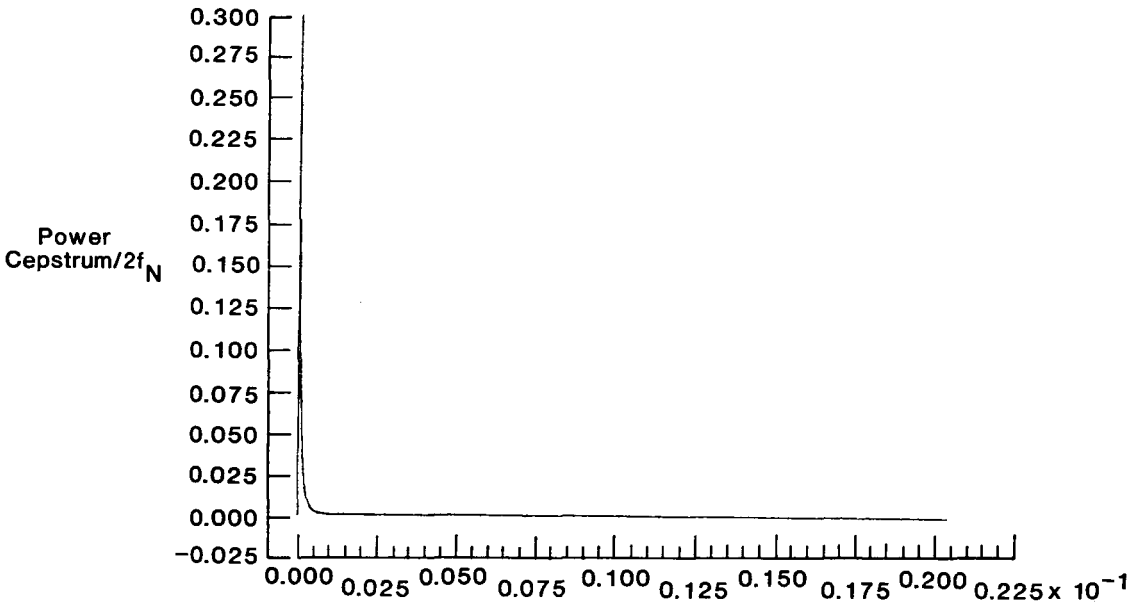

(c) Power cepstrum.

Figure 2.- Concluded.

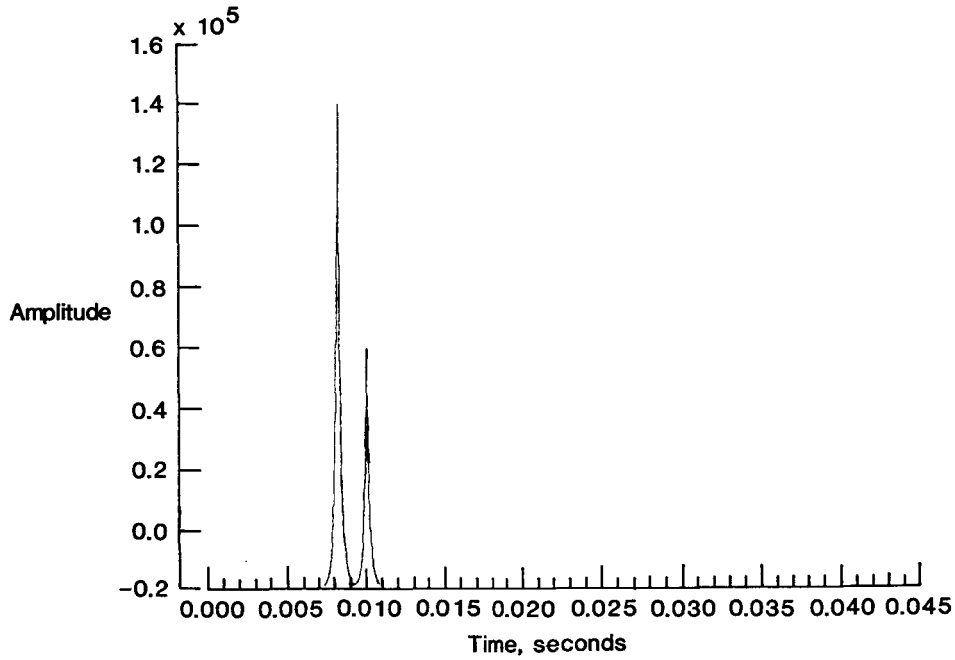

(a) Time history.

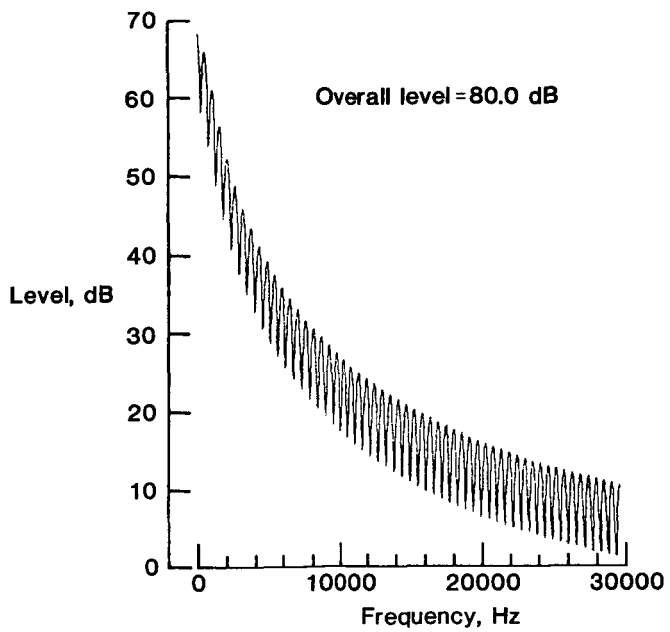

(b) Power spectrum.

Figure 3.- Exponential signal with one ideal echo (α = 0.5 and t_e = 0.0018 sec).

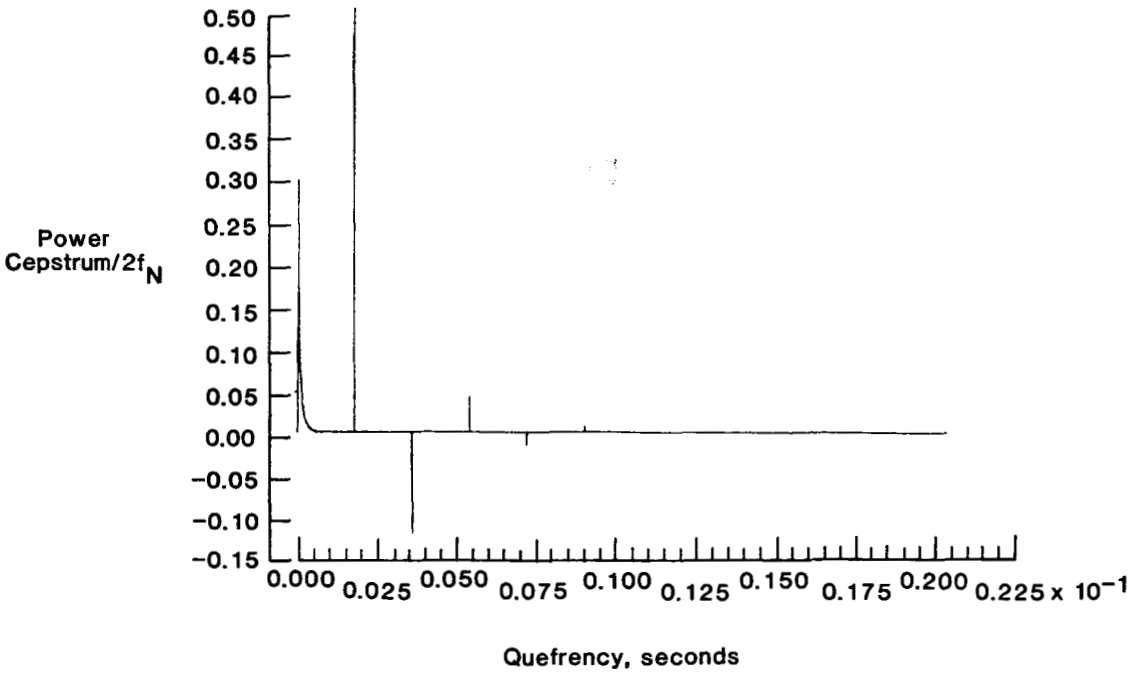

(c) Power cepstrum.

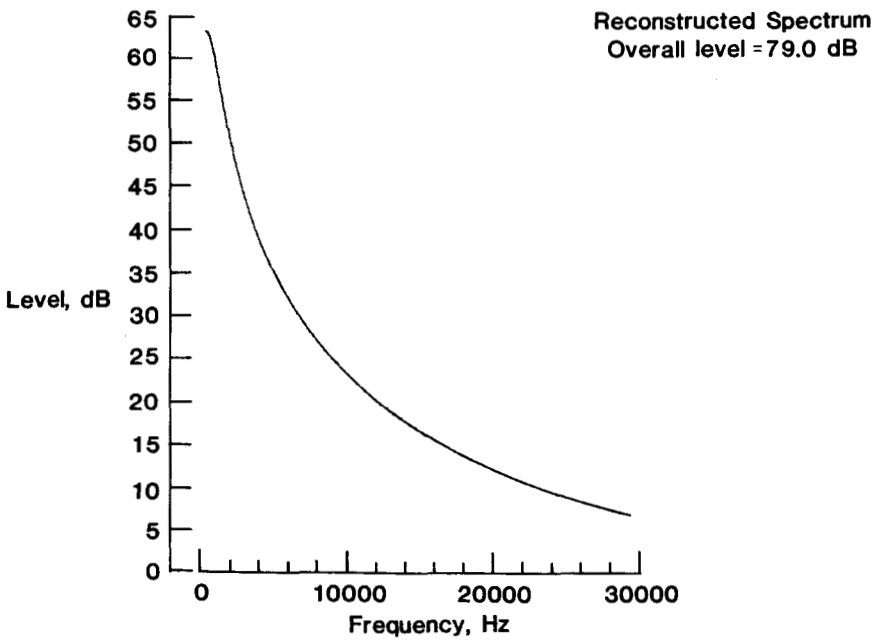

(d) Reconstructed power spectrum.

Figure 3.- Continued.

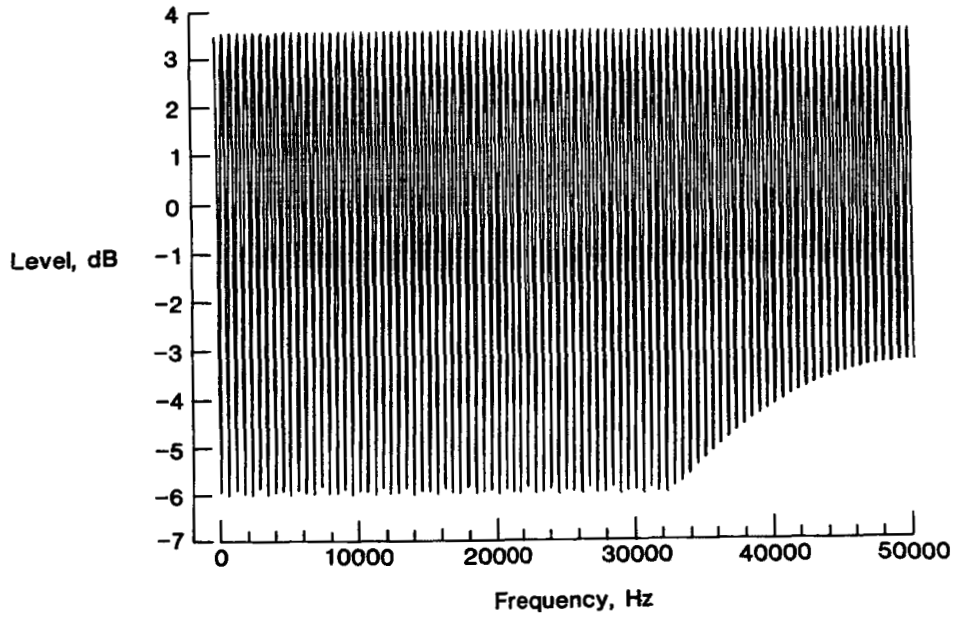

(e) Spectral correction.

Figure 3.- Concluded.

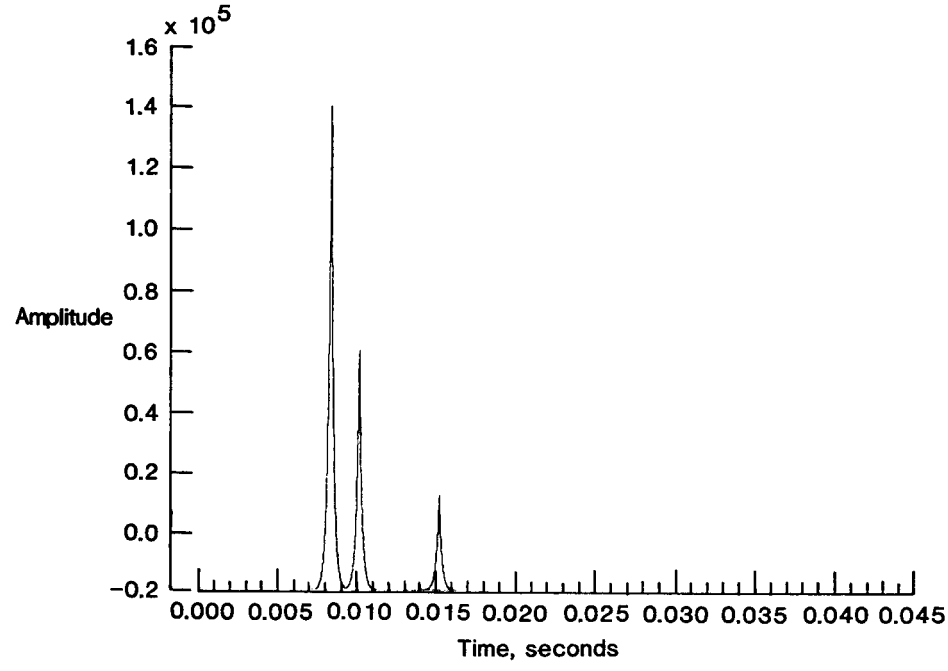

(a) Time history.

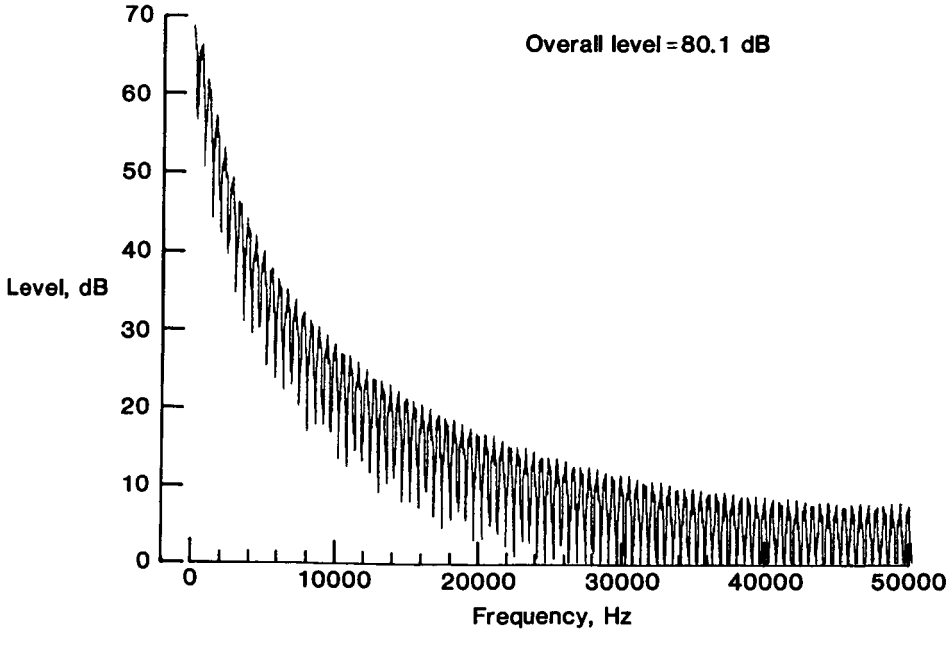

(b) Power spectrum.

Figure 4.- Exponential signal with two ideal echoes (α = 0.5, t_1 = 0.0018 sec, β = 0.2, and t_2 = 0.0068 sec).

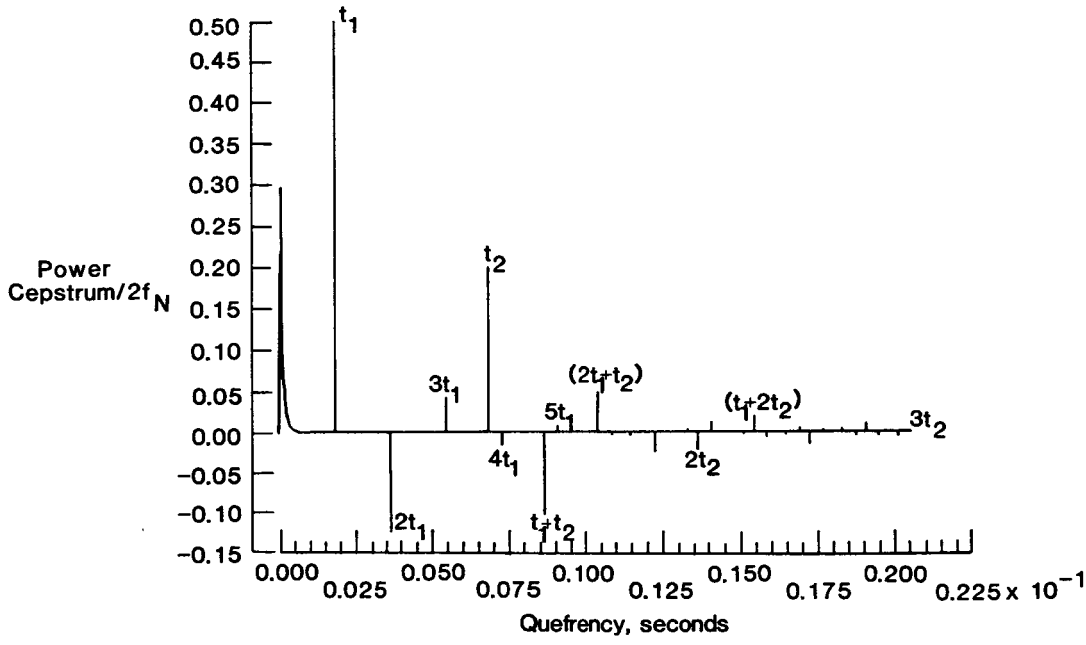

(c) Power cepstrum.

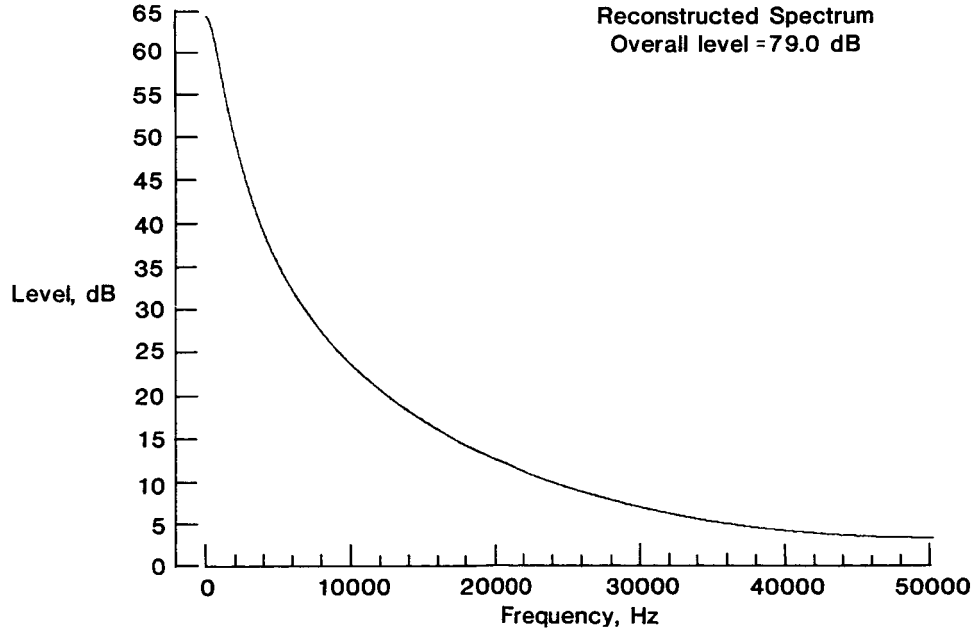

(d) Reconstructed power spectrum.

Figure 4.- Concluded.

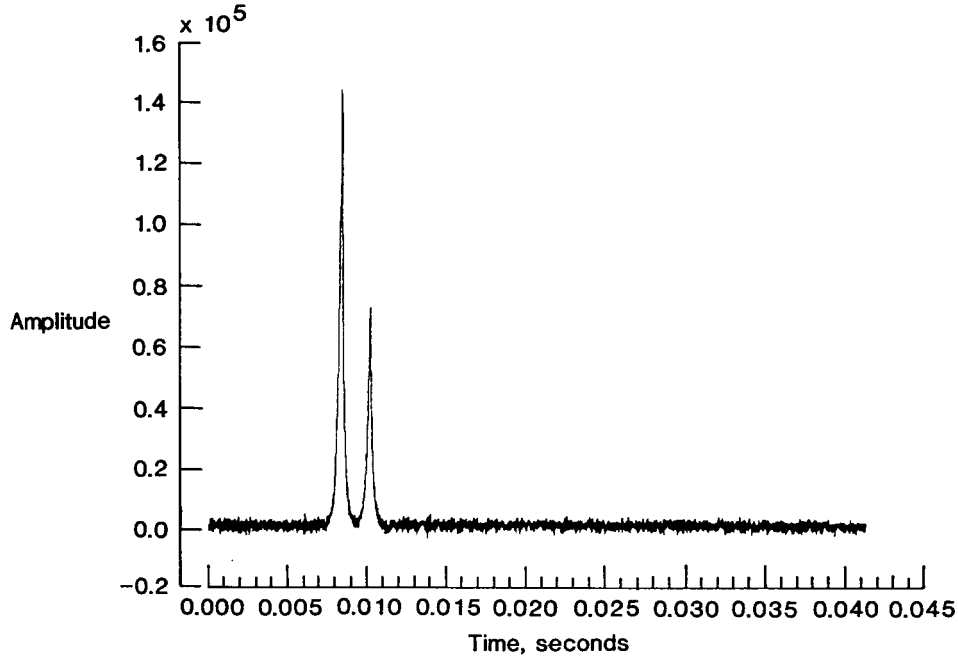

(a) Time history.

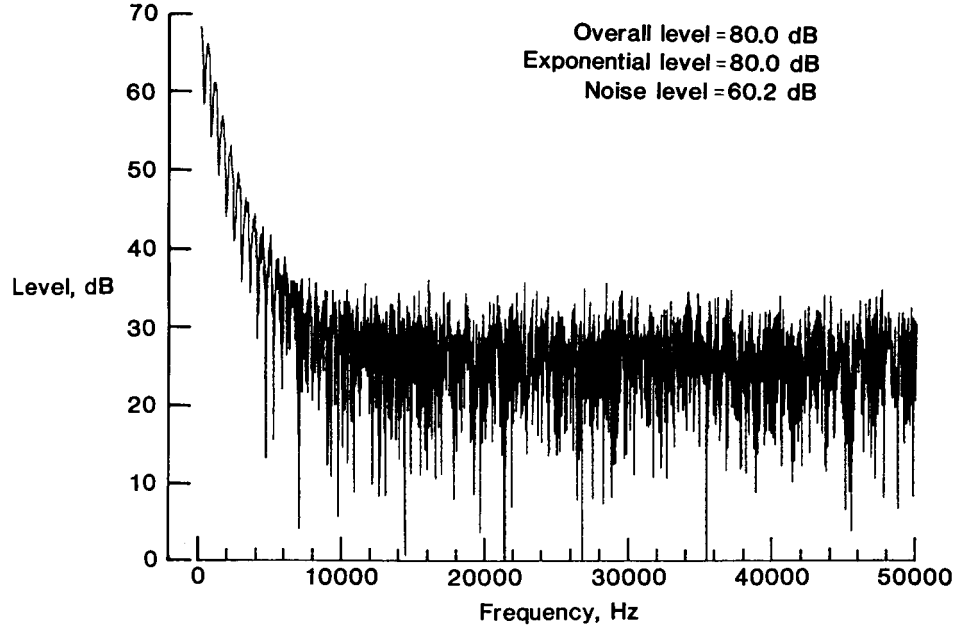

(b) Power spectrum.

Figure 5.- Exponential signal with one ideal echo (α = 0.5 and t_e = 0.0018 sec) and 60 dB of additive noise.

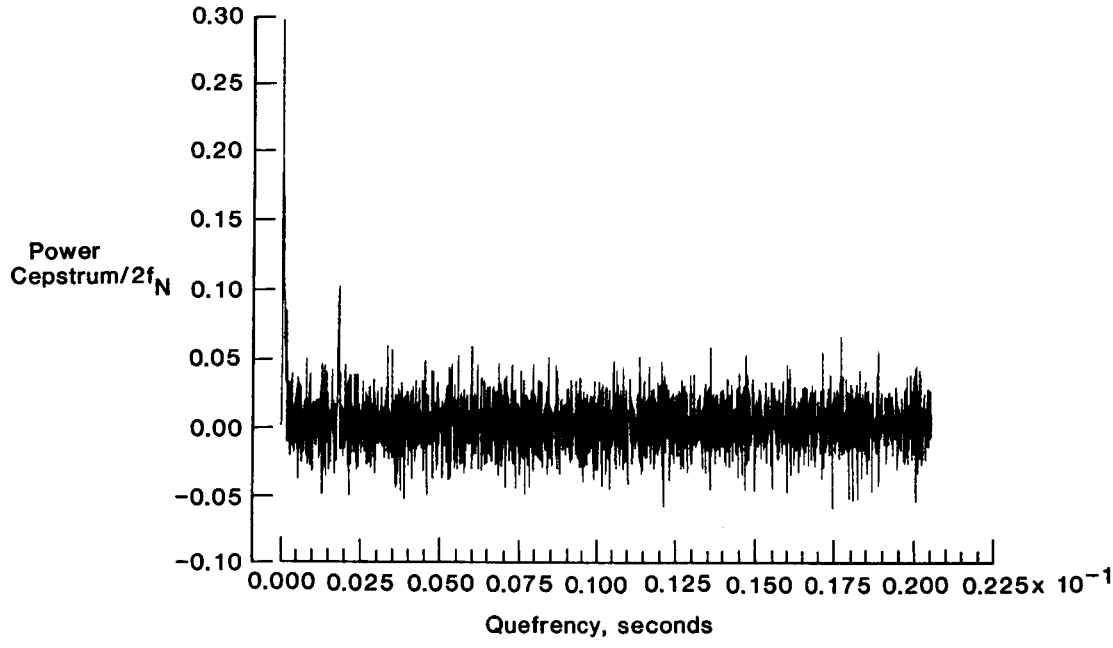

(c) Power cepstrum.

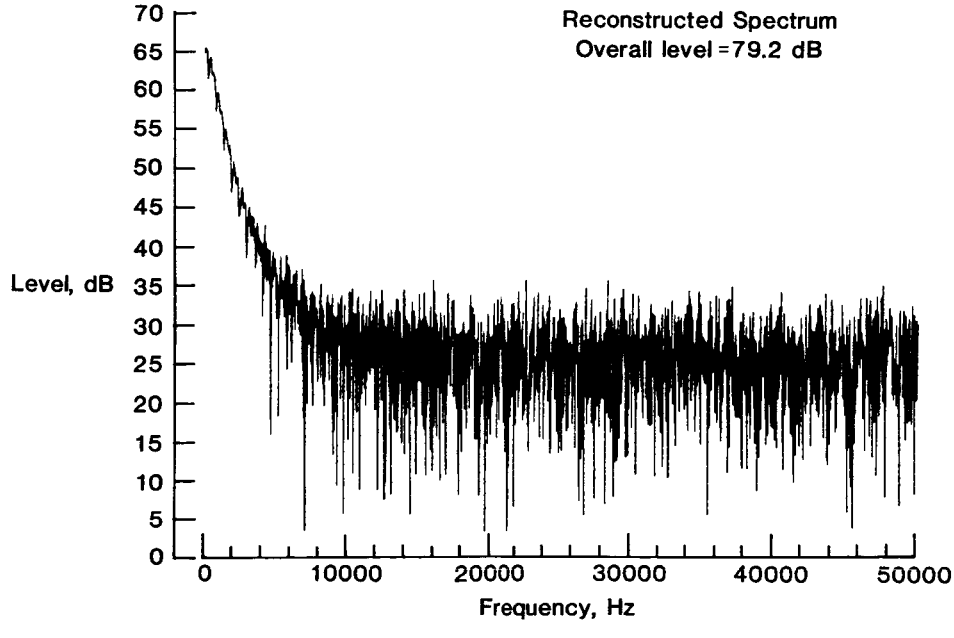

(d) Reconstructed power spectrum.

Figure 5.- Concluded.

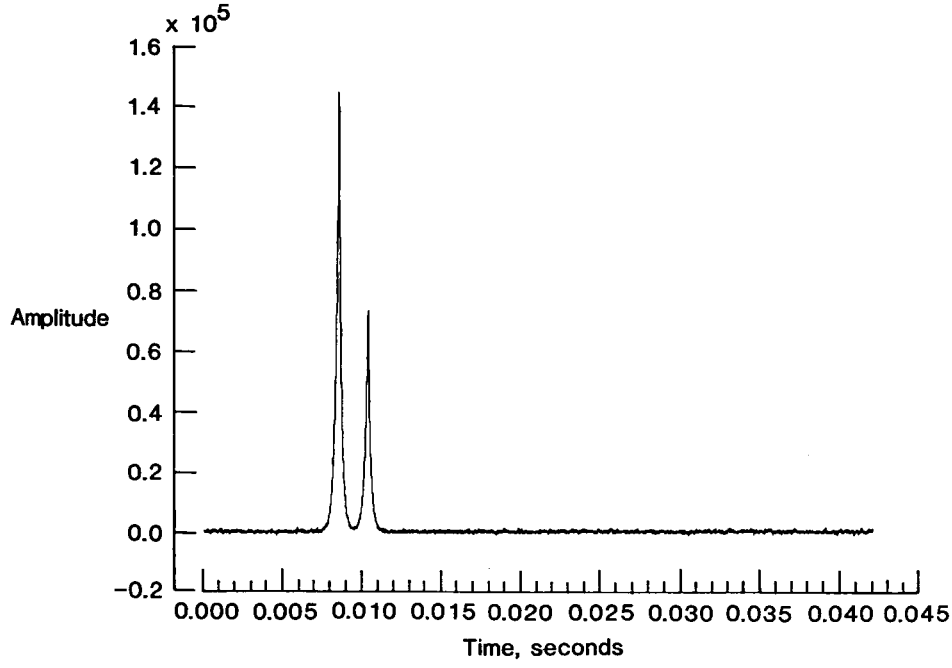

(a) Time history.

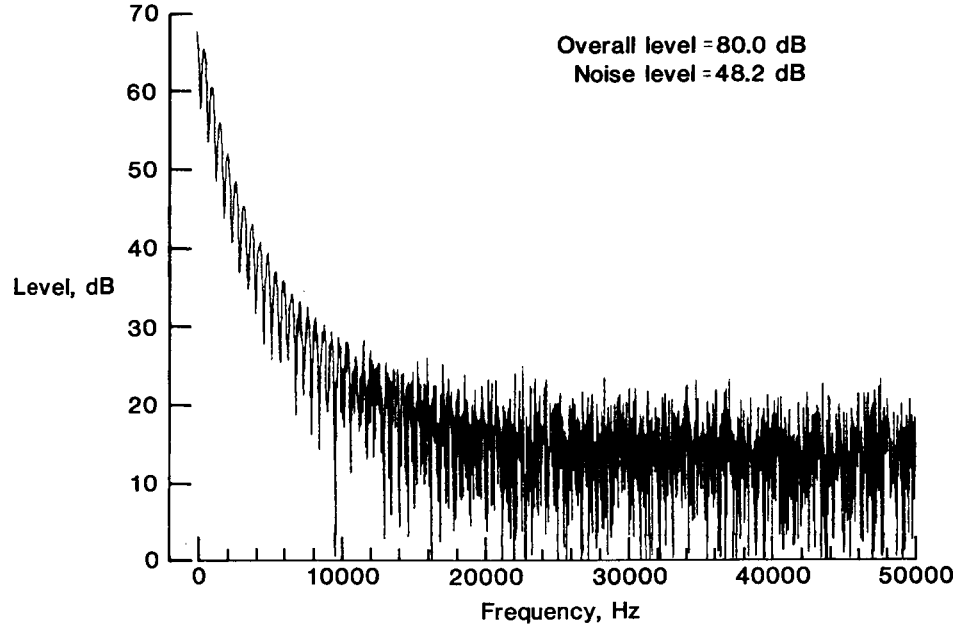

(b) Power spectrum.

Figure 6.- Exponential signal with one ideal echo (α = 0.5 and t_e = 0.0018 sec) and 48 dB of additive noise.

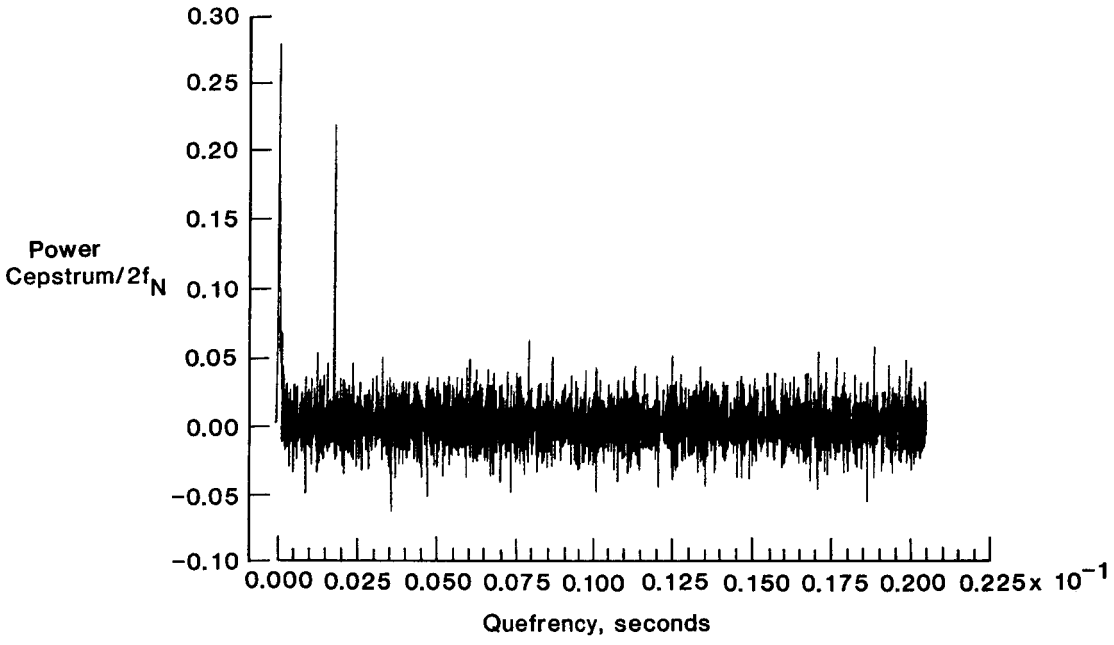

(c) Power cepstrum.

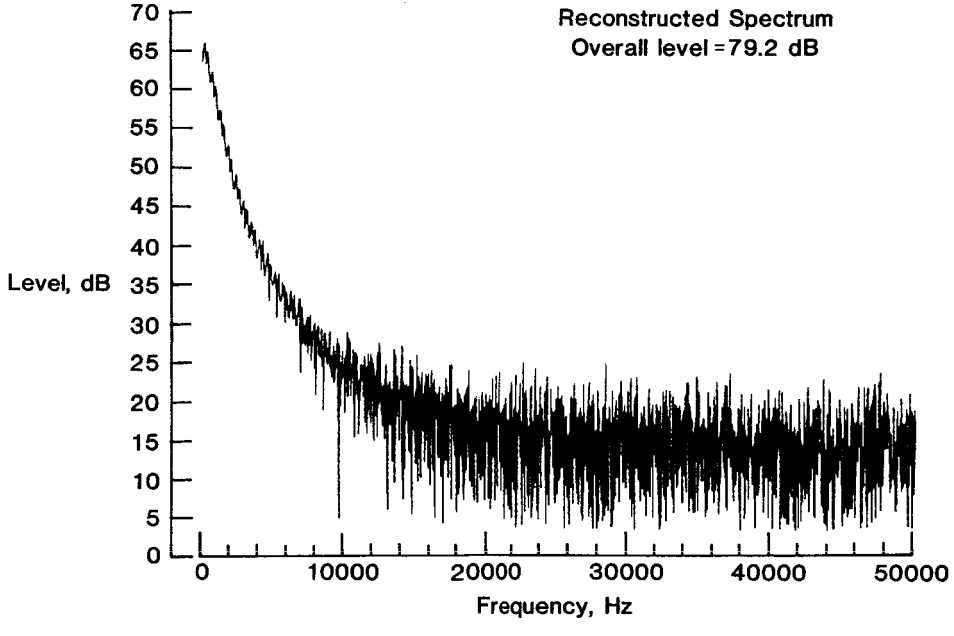

(d) Reconstructed power spectrum.

Figure 6.- Concluded.

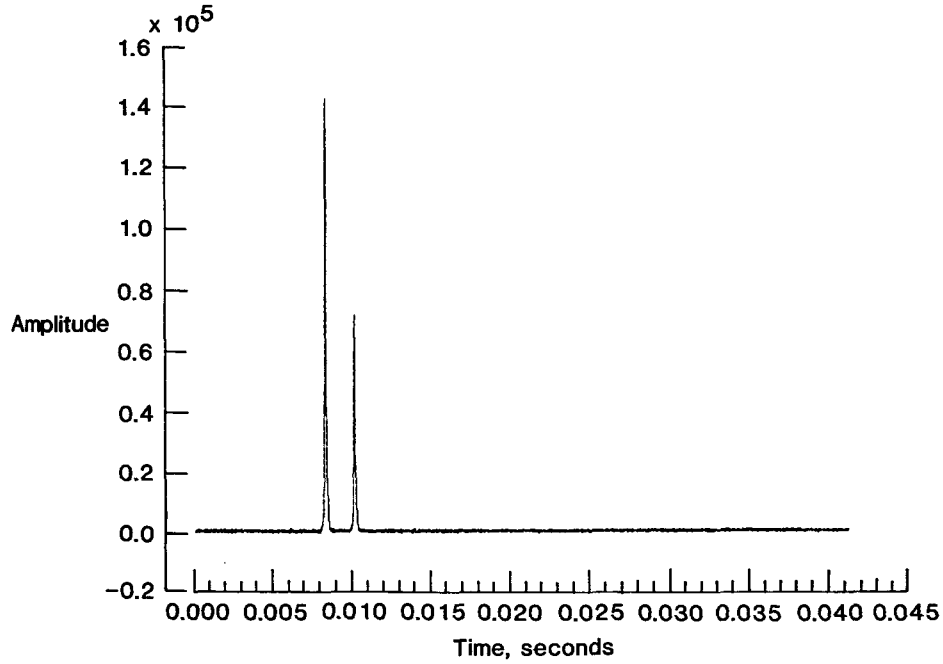

(a) Time history.

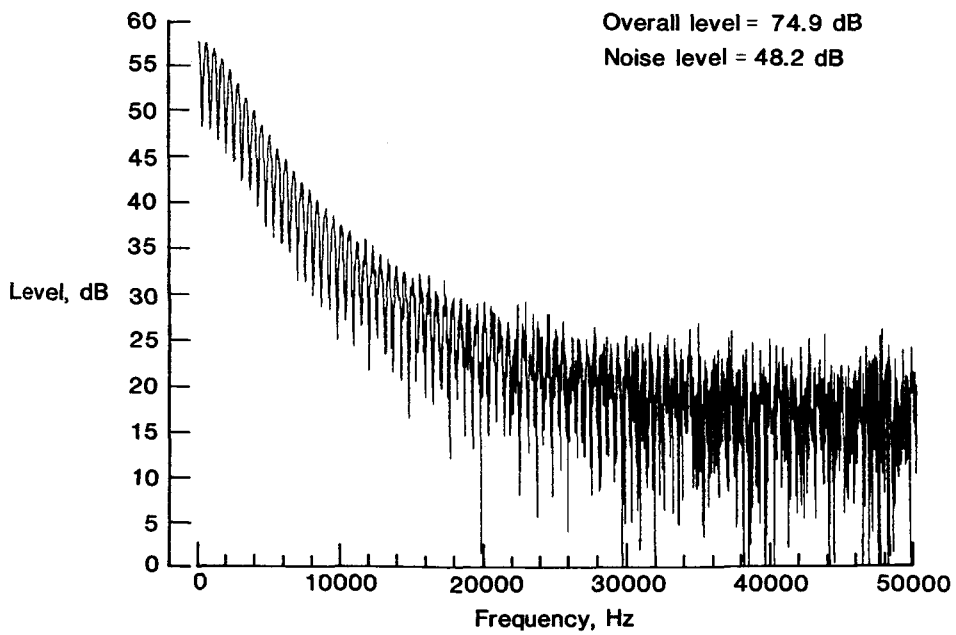

(b) Power spectrum.

Figure 7.- Exponential signal for $k = 20\ 000$ with one ideal echo ($\alpha = 0.5$ and $t_e = 0.0018$ sec) and 48 dB of additive noise.

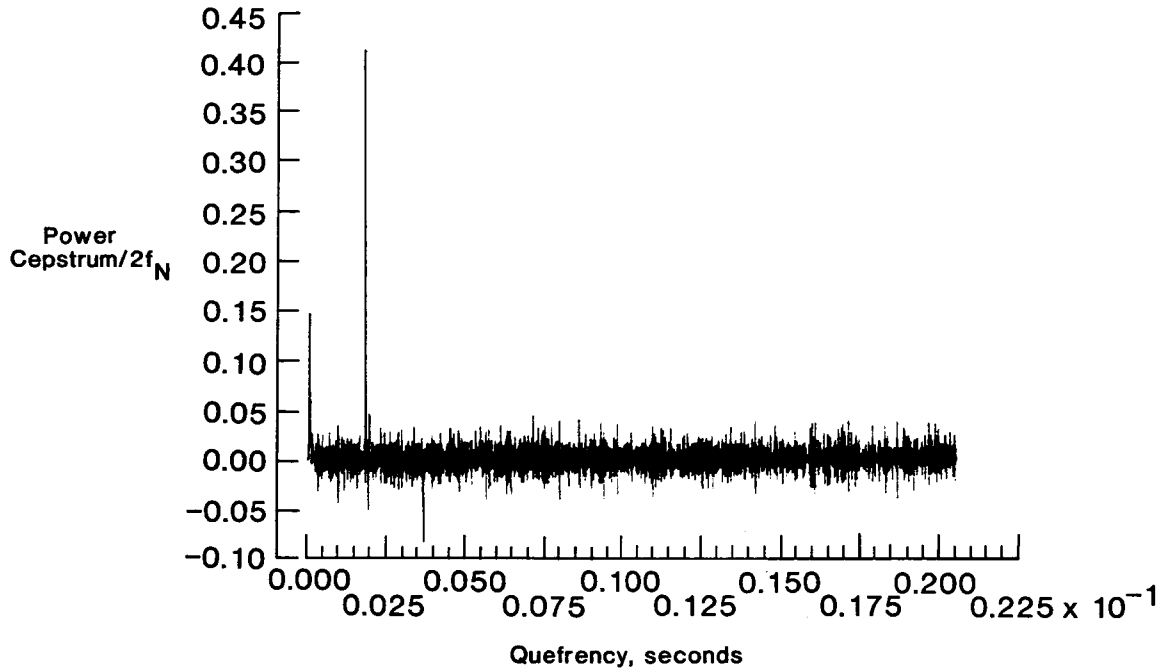

(c) Power cepstrum.

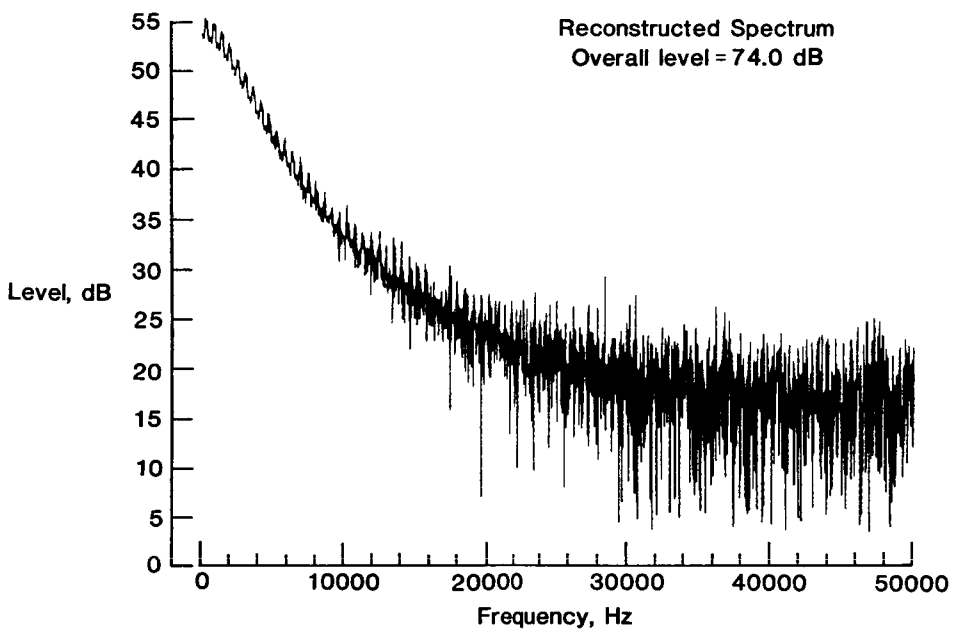

(d) Reconstructed power spectrum.

Figure 7.- Concluded.

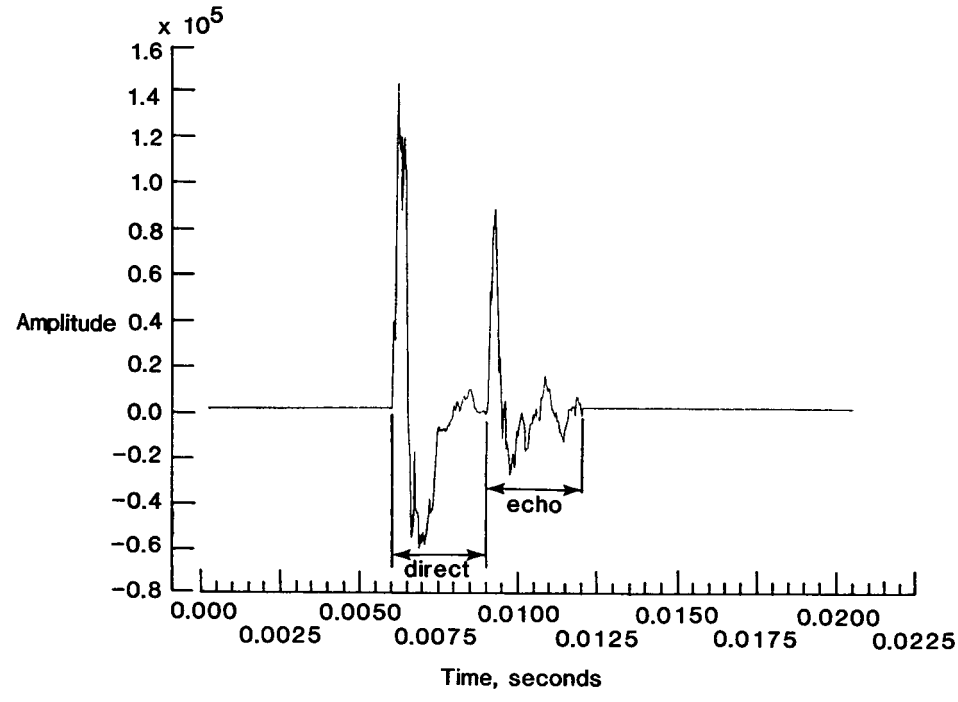

(a) Time history.

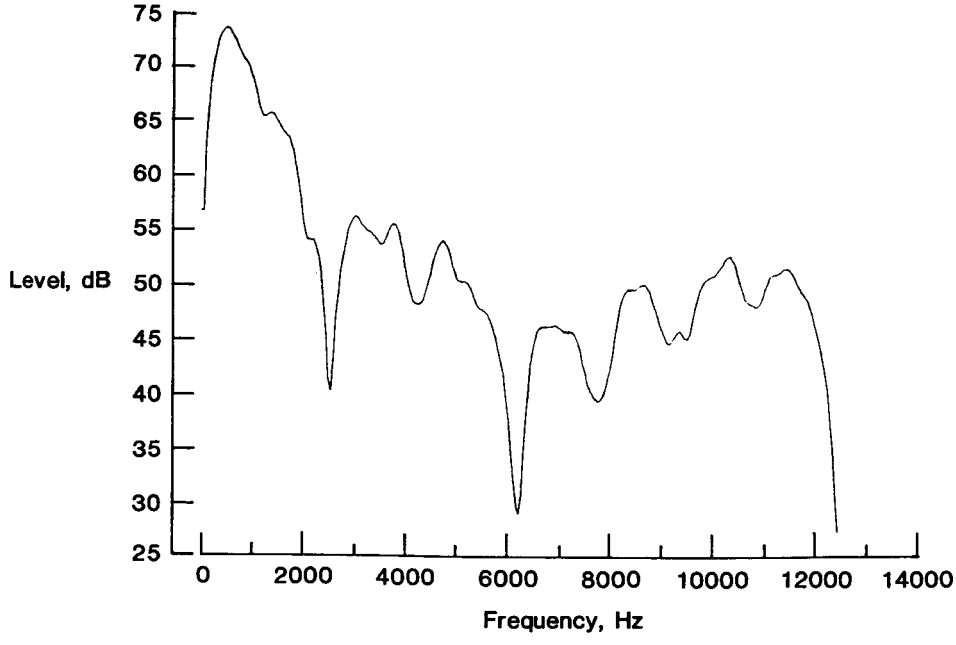

(b) Power spectrum of direct signal.

Figure 8.- Impulsive signal with one echo.

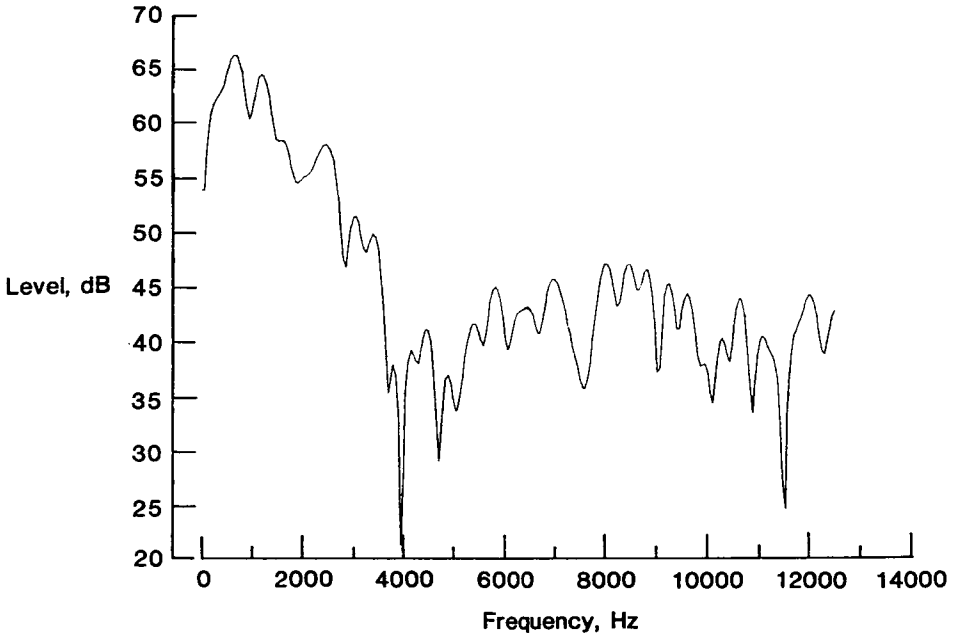

(c) Power spectrum of echoed signal.

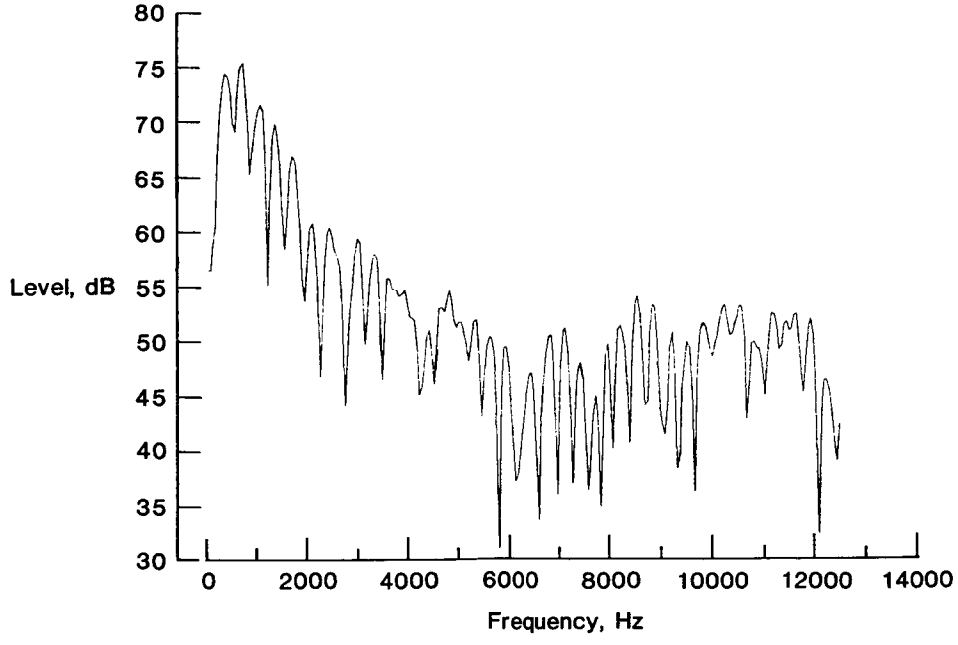

(d) Power spectrum of direct plus echoed signal.

Figure 8.- Concluded.

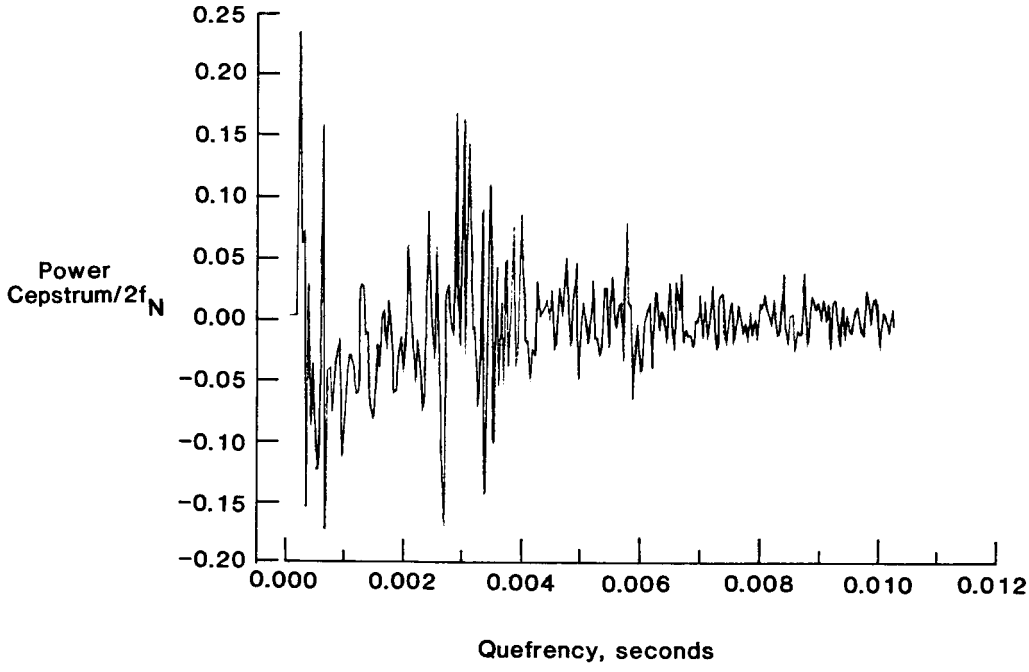

(a) Power cepstrum of direct signal with echo.

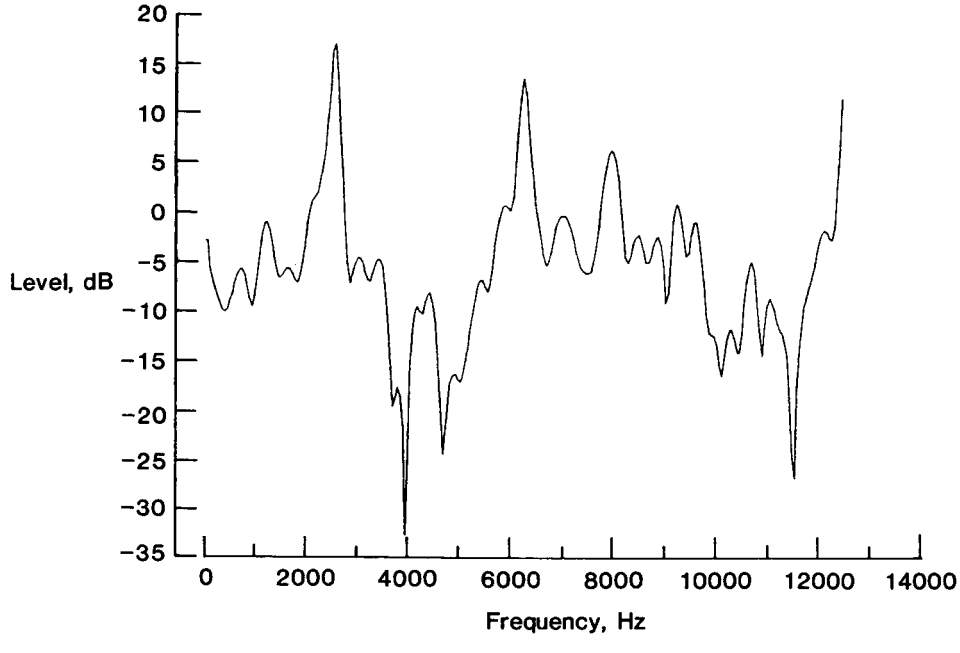

(b) Function $|H(f)|^2$.

Figure 9.- Correction of contaminated data of figure 8(a).

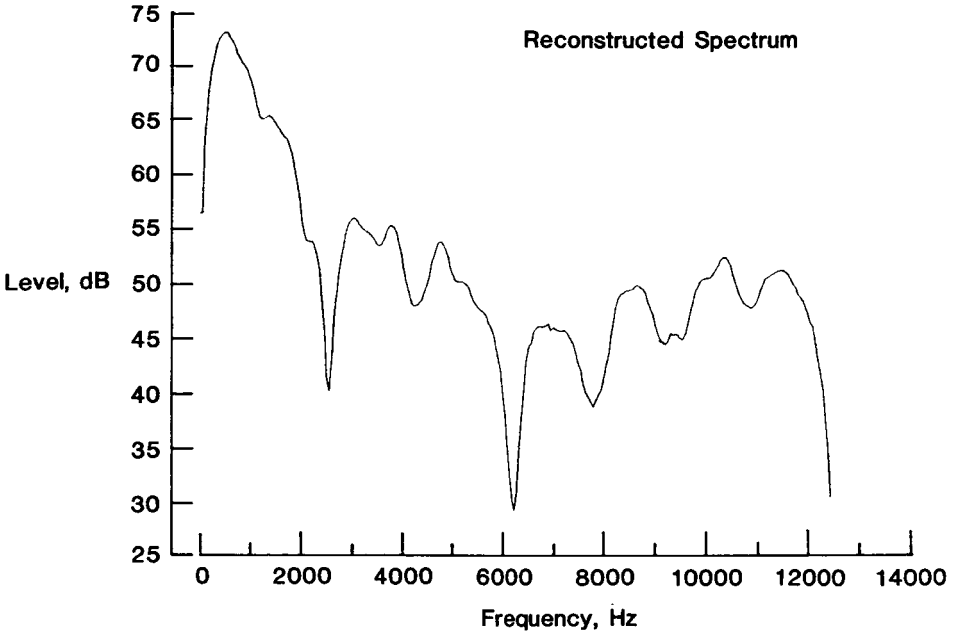

(c) Reconstructed power spectrum found from correction for H(f) and t_e.

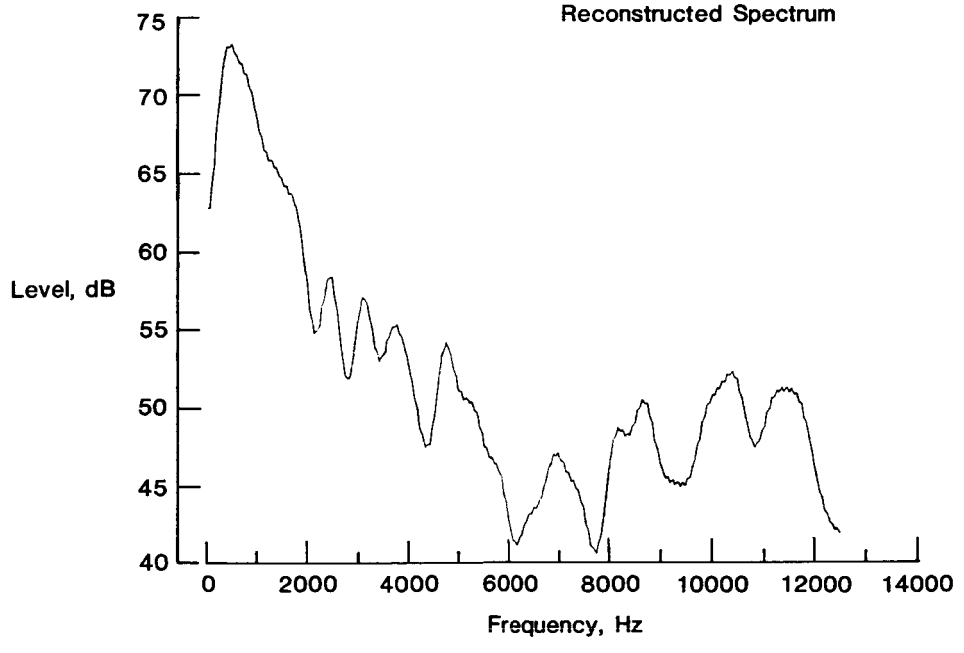

(d) Reconstructed power spectrum found from editing of power cepstrum.

Figure 9.- Concluded.

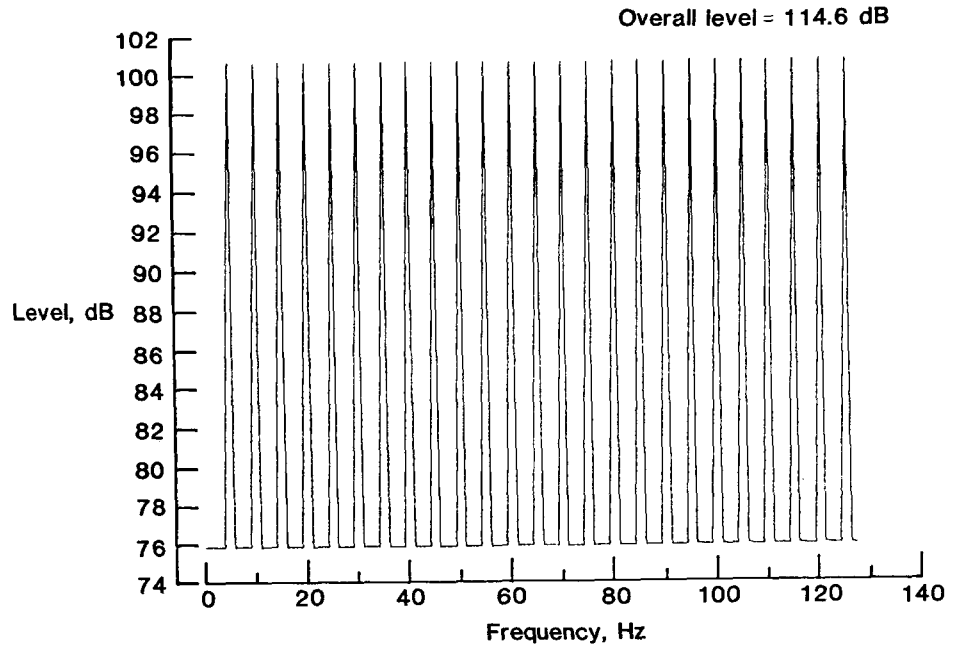

(a) Power spectrum.

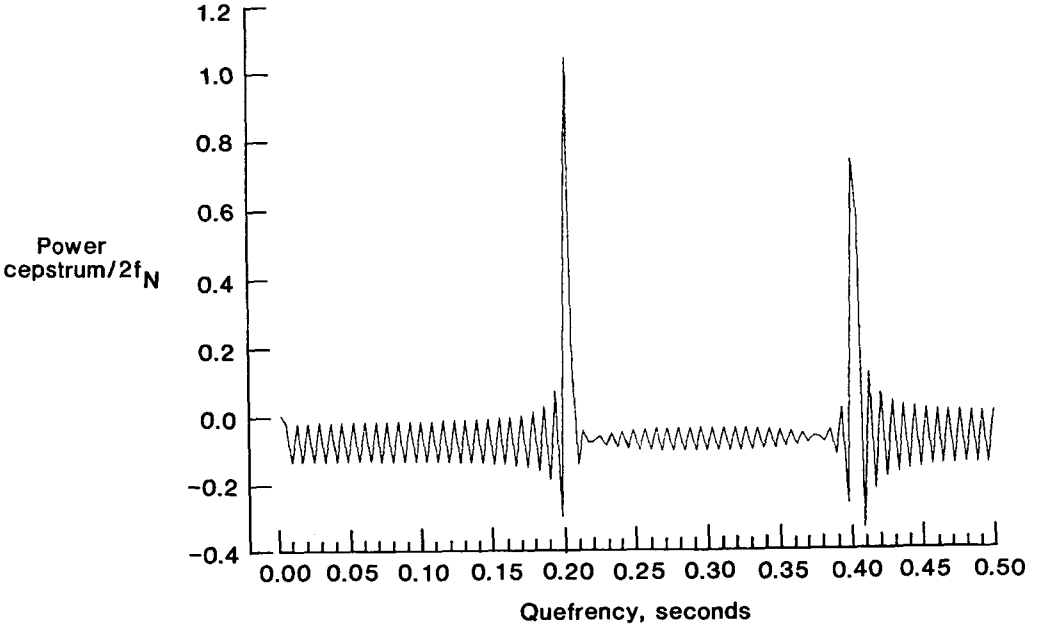

(b) Power cepstrum.

Figure 10.- Periodic signal without echo. Off-harmonic level is source related. f_f = 5 Hz.

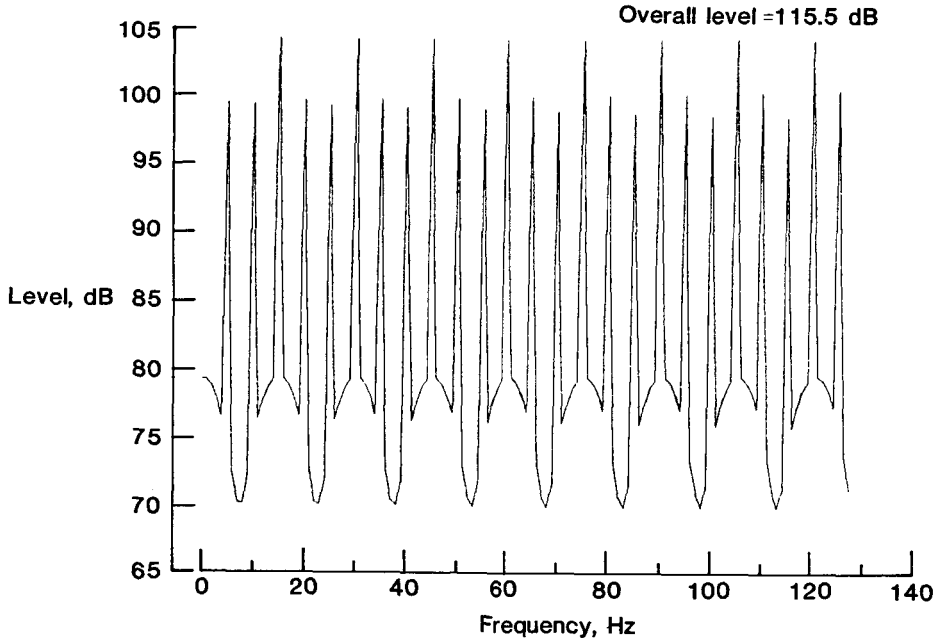

(a) Power spectrum.

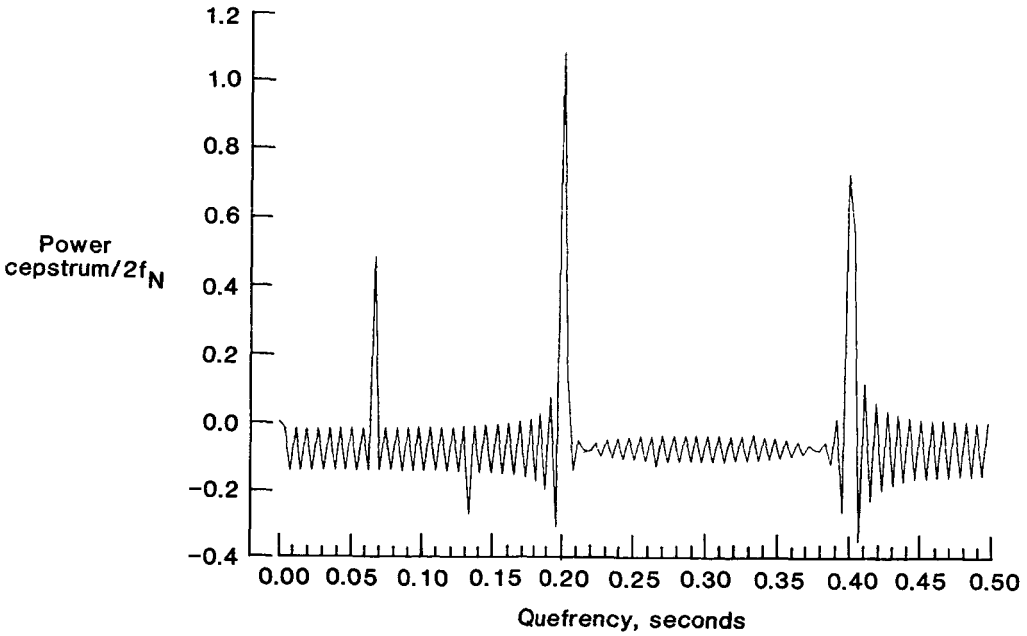

(b) Power cepstrum.

Figure 11.- Periodic signal with one ideal echo (α = 0.5 and t_e = 0.7 sec) for source-related off-harmonic level.

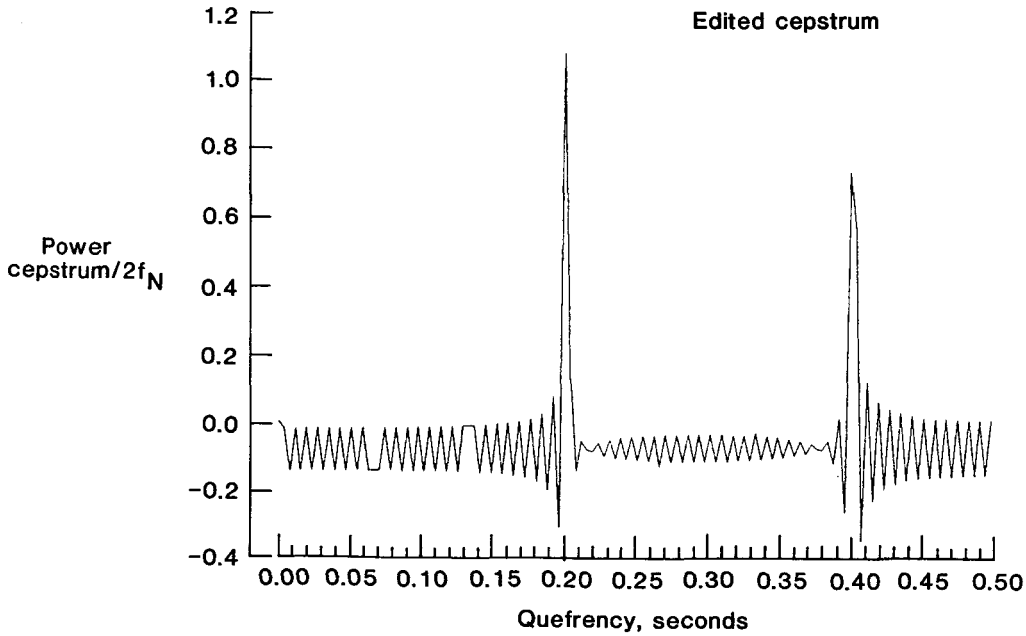

(c) Edited power cepstrum.

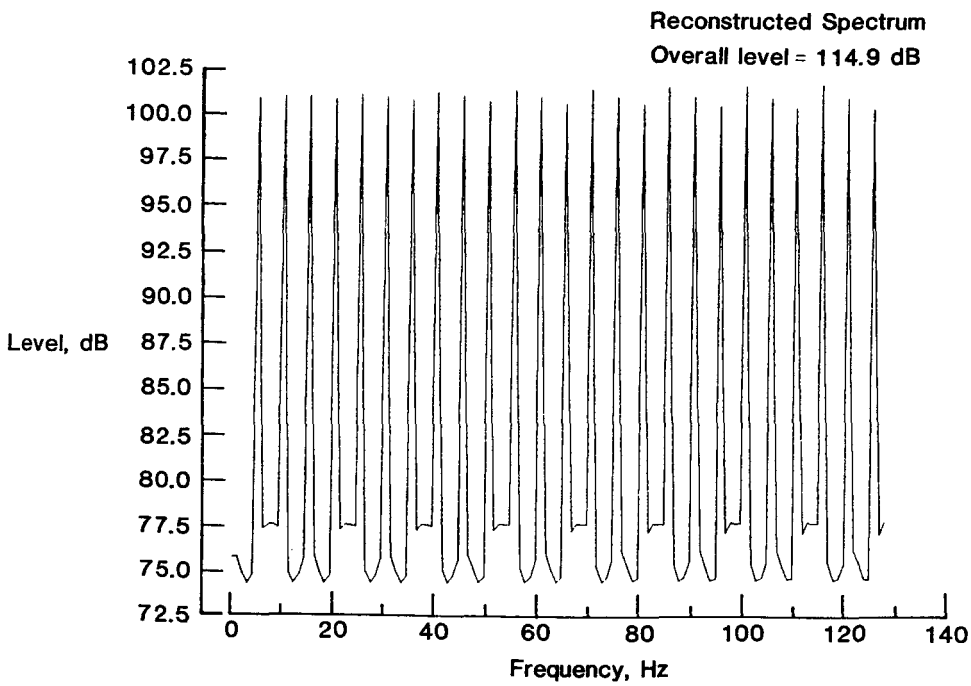

(d) Reconstructed power spectrum.

Figure 11.- Concluded.

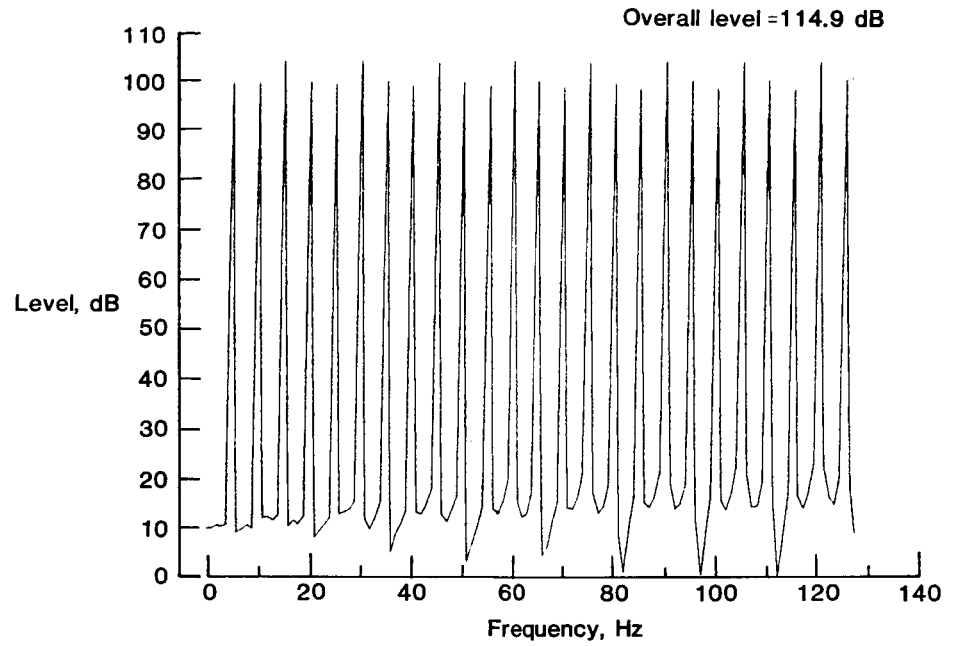

(a) Power spectrum.

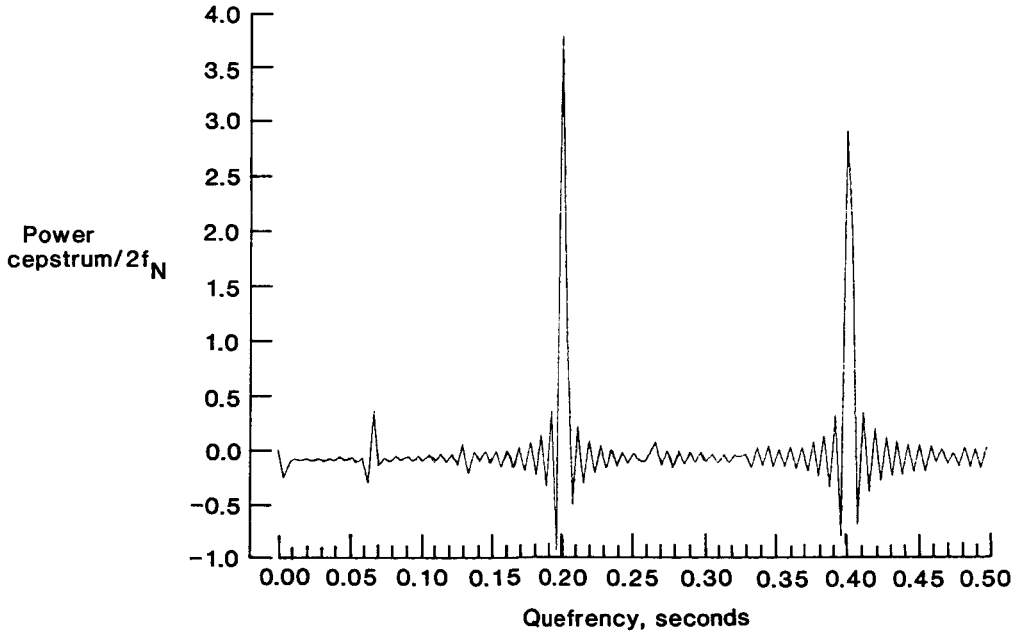

(b) Power cepstrum.

Figure 12.- Periodic signal with one ideal echo (α = 0.5 and t_e = 0.07 sec) for no off-harmonic energy.

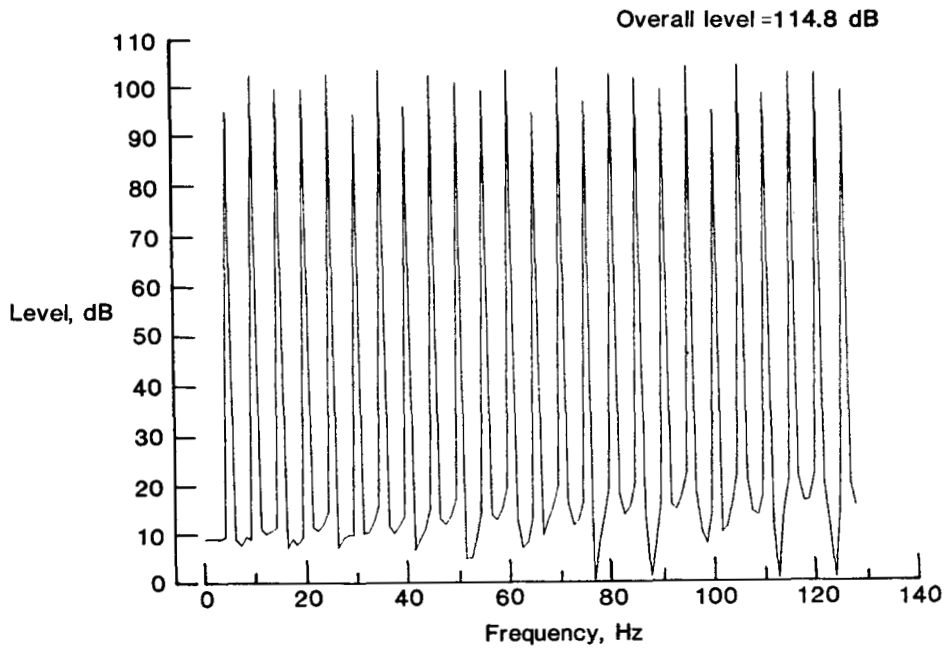

(a) Power spectrum.

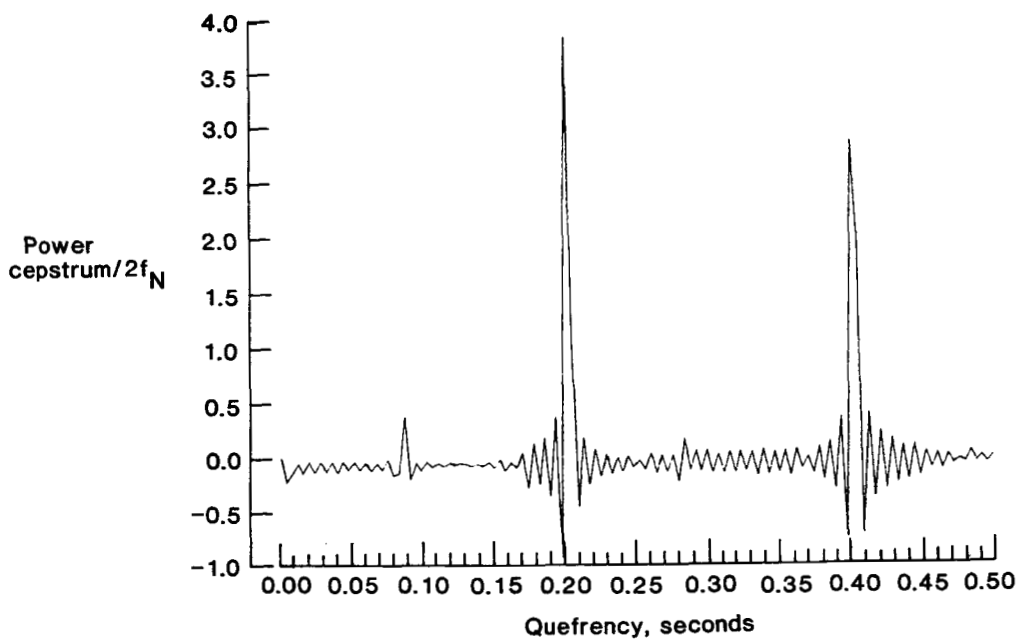

(b) Power cepstrum.

Figure 13.- Periodic signal with one ideal echo (α = 0.5 and t_e = 0.29 sec) for no off-harmonic energy.

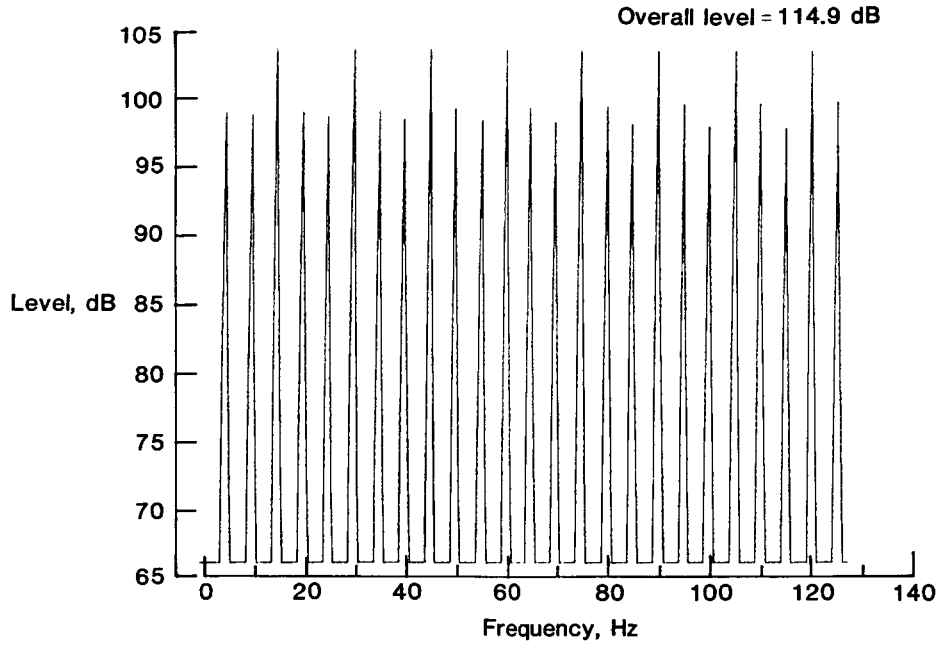

(a) Power spectrum.

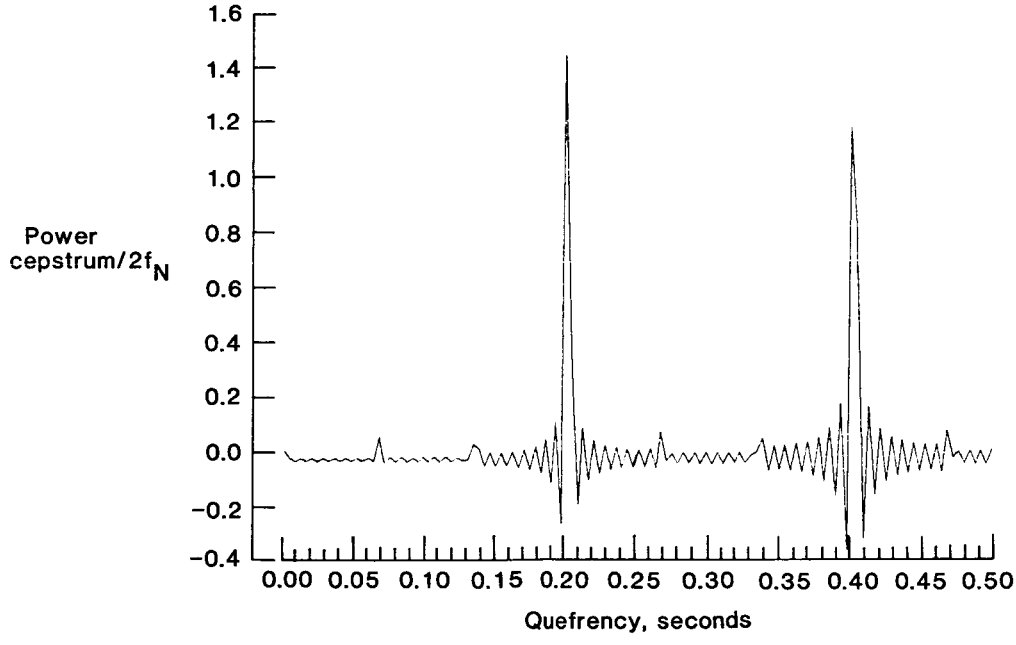

(b) Power cepstrum.

Figure 14.- Periodic signal with one ideal echo (α = 0.5 and t_e = 0.07 sec) for non-source-related off-harmonic level.

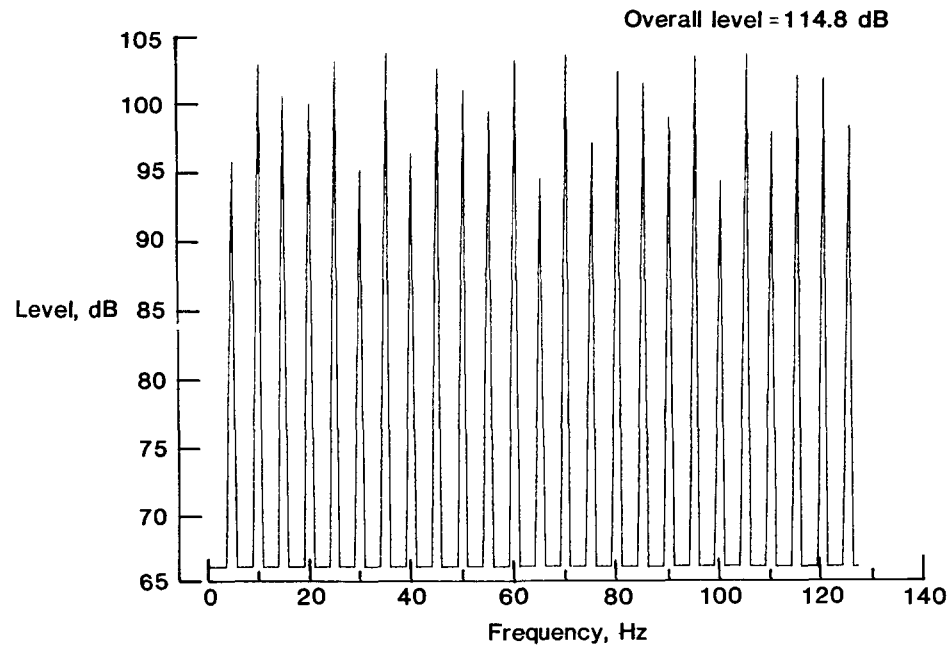

(a) Power spectrum.

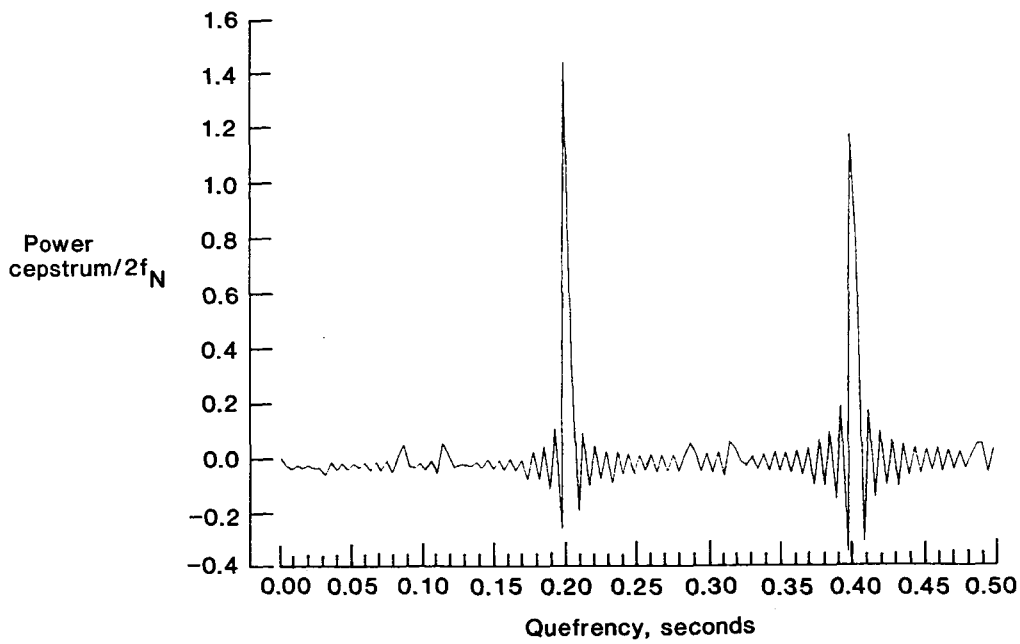

(b) Power cepstrum.

Figure 15.- Periodic signal with one ideal echo (α = 0.5 and t_e = 0.29 sec) for non-source-related off-harmonic level.

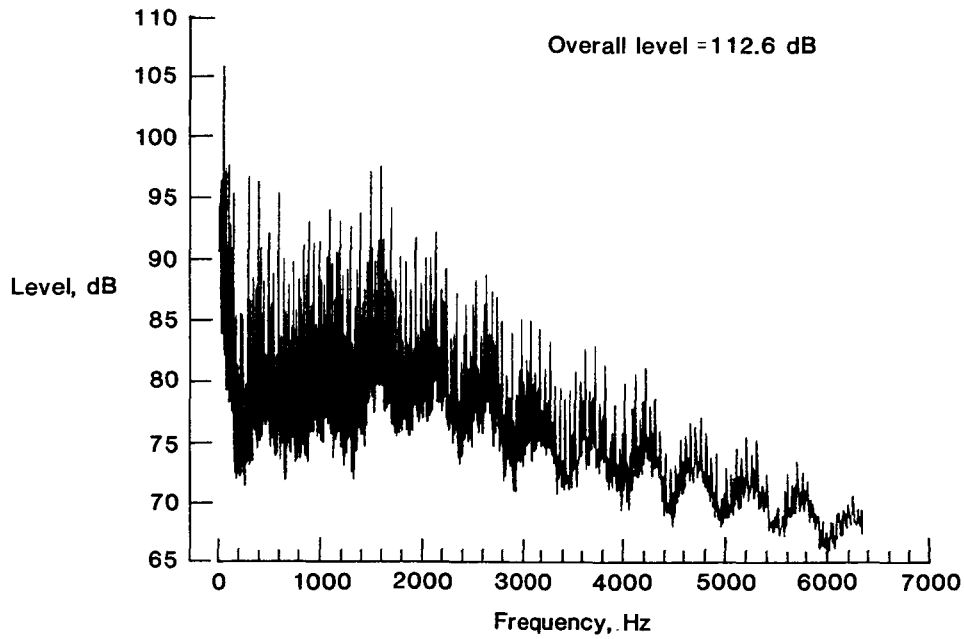

(a) Power spectrum (power-averaged spectrum).

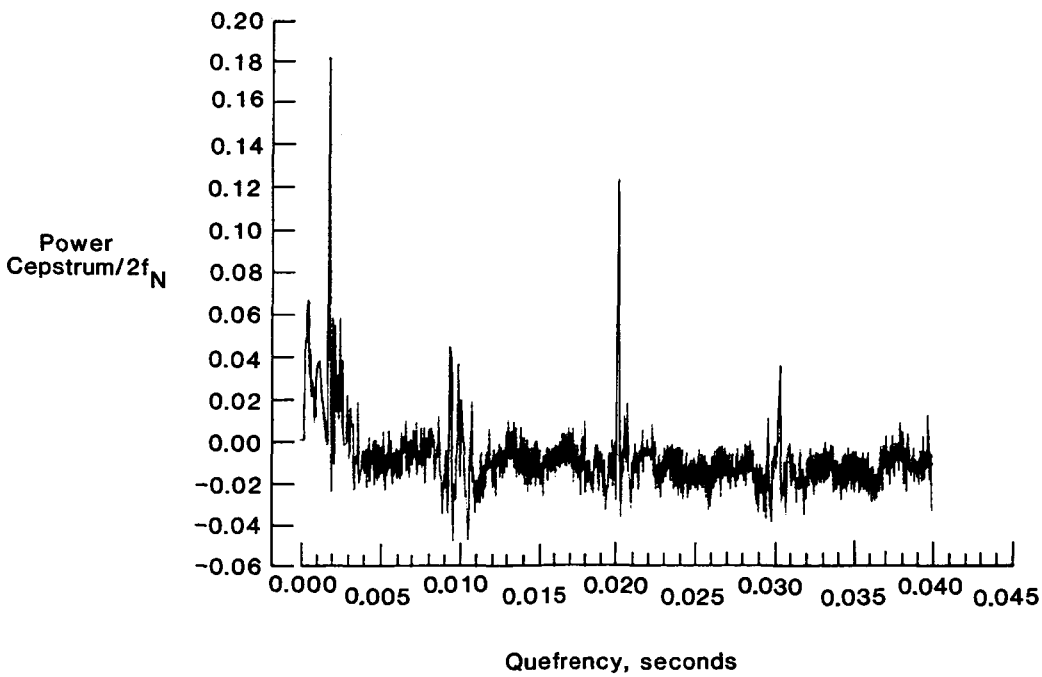

(b) Power cepstrum.

Figure 16.- Model-scale helicopter-rotor acoustic data for velocity of 60 knots, rotor angle of attack of 2°, and rotor thrust coefficient of 0.007. f_{BP} = 100 Hz; microphone 3.

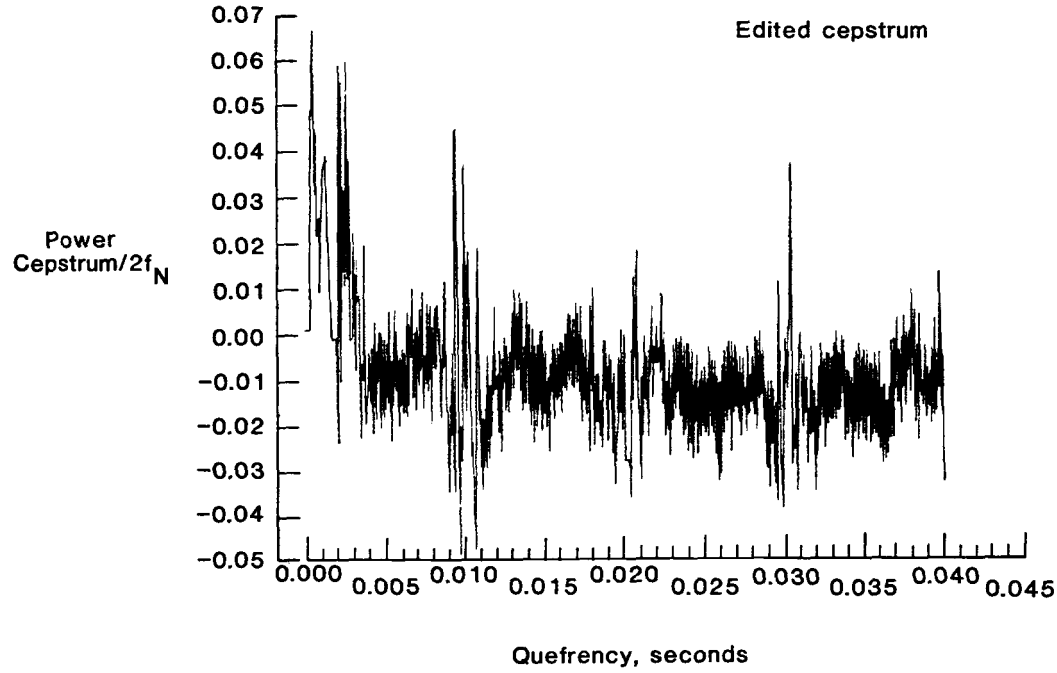

(c) Edited power cepstrum.

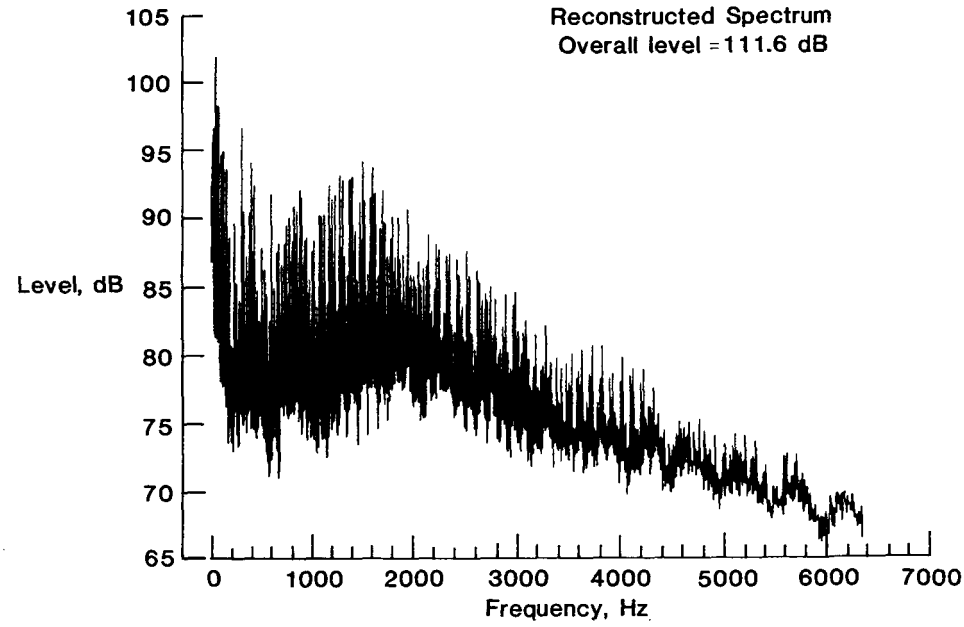

(d) Reconstructed power spectrum.

Figure 16.- Continued.

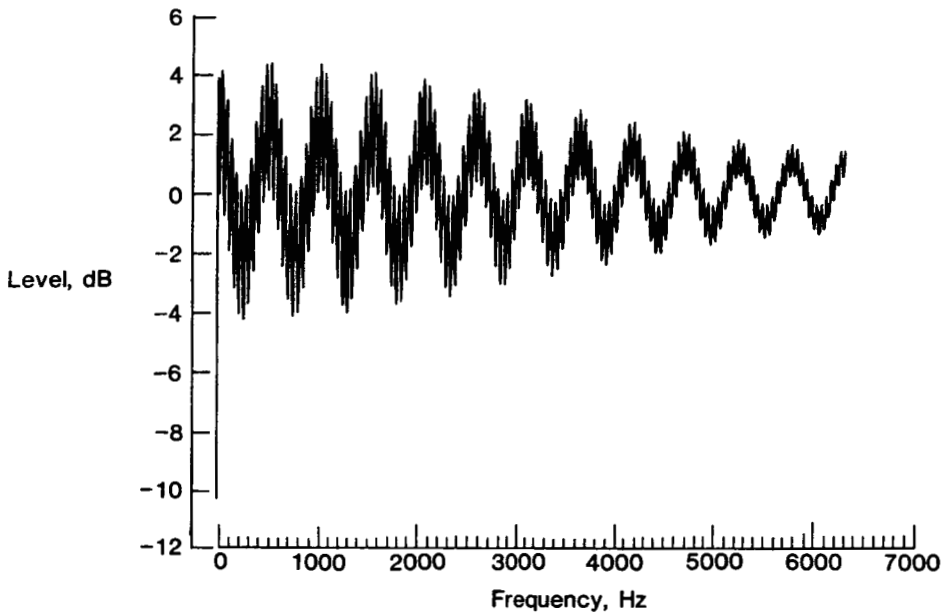

(e) Spectral correction.

Figure 16.- Concluded.

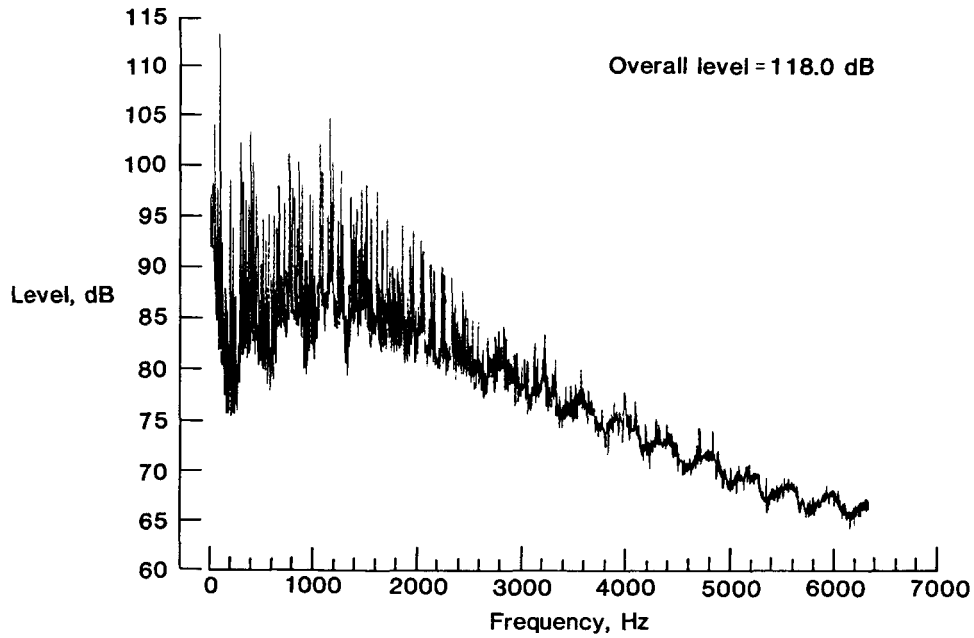

(a) Power spectrum.

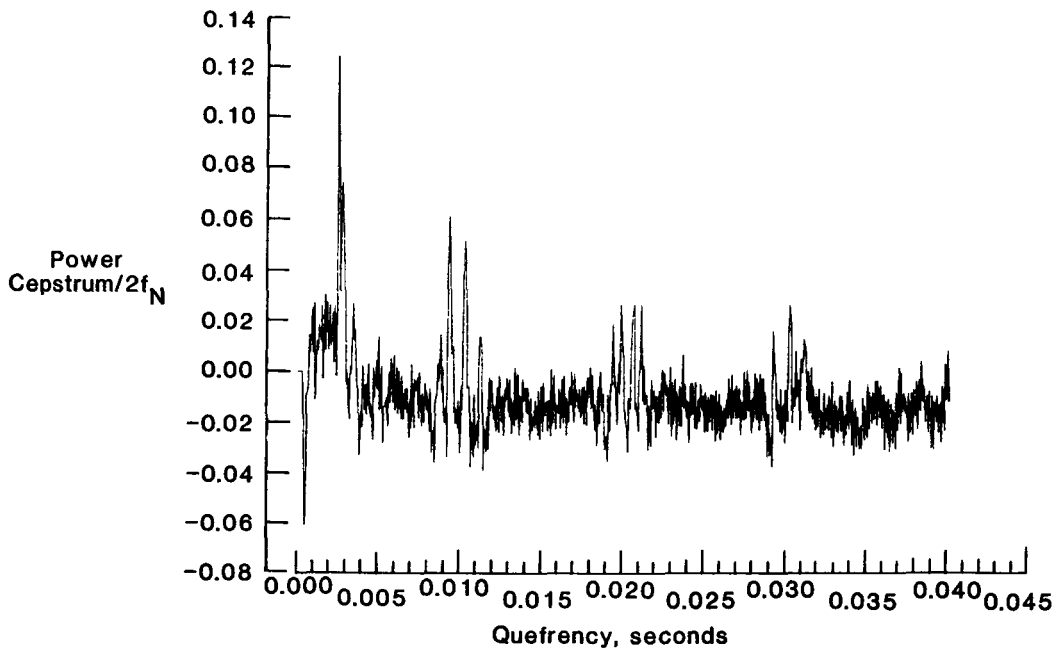

(b) Power cepstrum.

Figure 17.- Model-scale helicopter-rotor acoustic data for velocity of 55 knots, rotor angle of attack of 6°, and rotor thrust coefficient of 0.007. f_{BP} = 100 Hz; microphone 2.

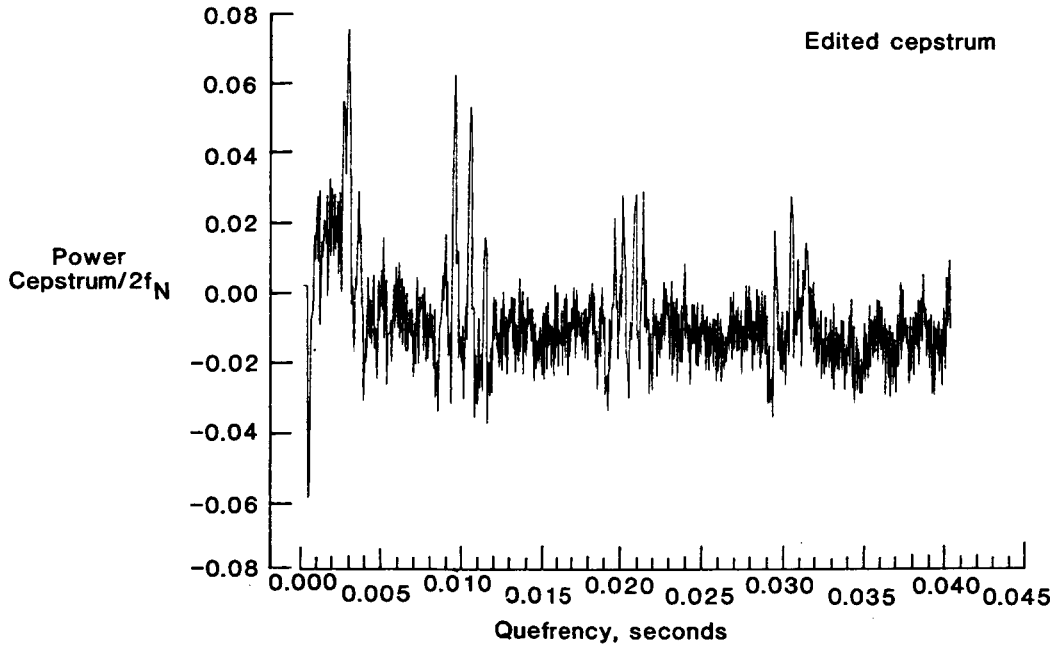

(c) Edited power cepstrum.

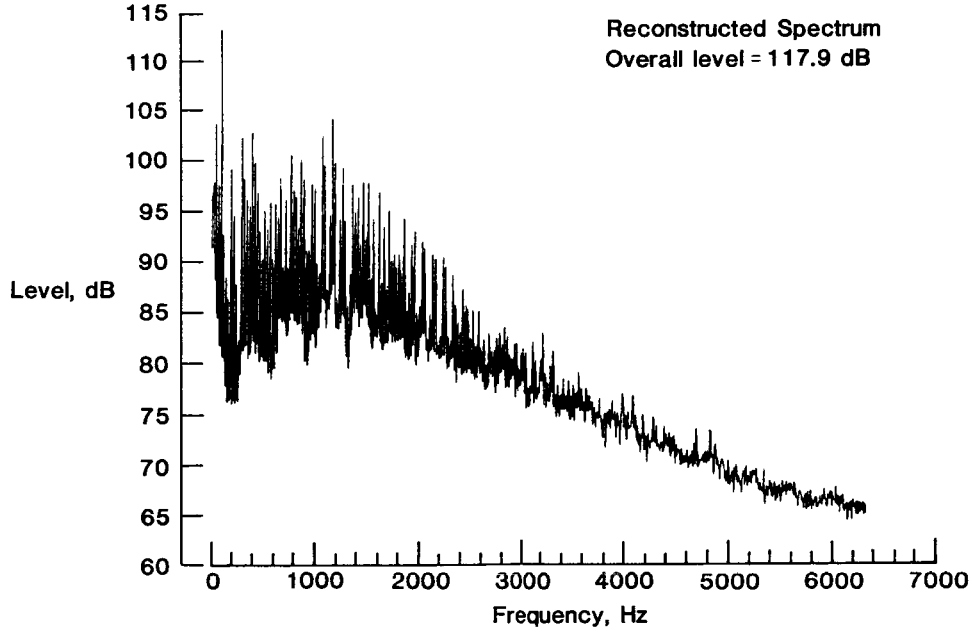

(d) Reconstructed power spectrum.

Figure 17.- Continued.

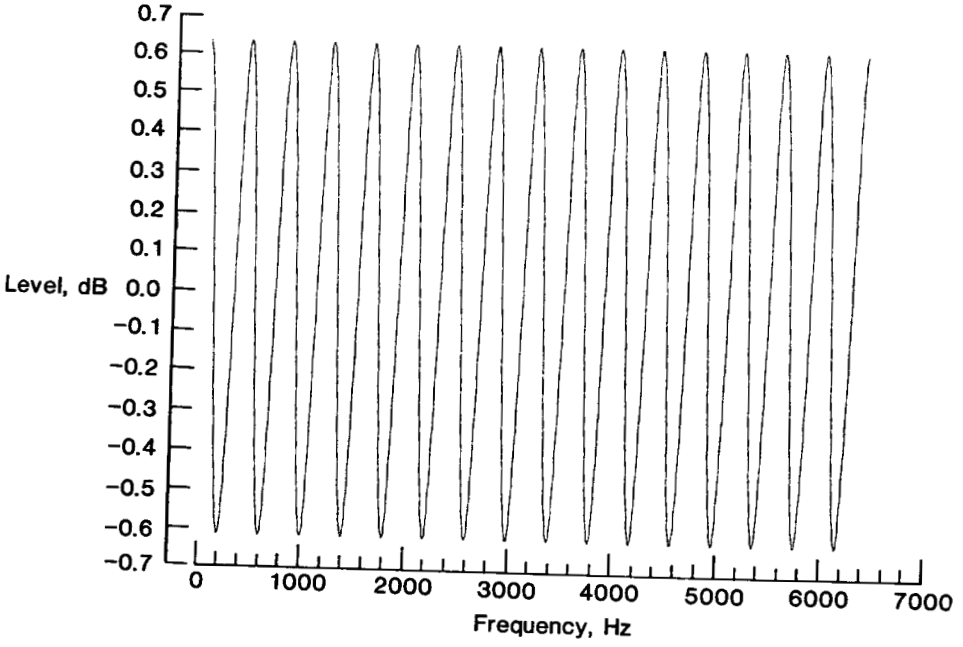

(e) Spectral correction.

Figure 17.- Concluded.

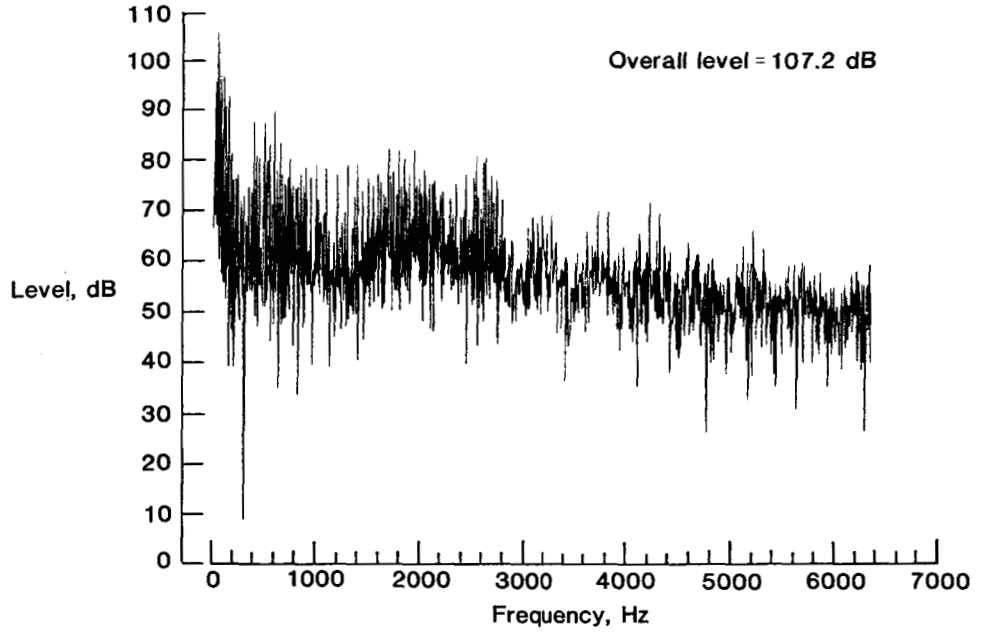

(a) Coefficient-averaged power spectrum.

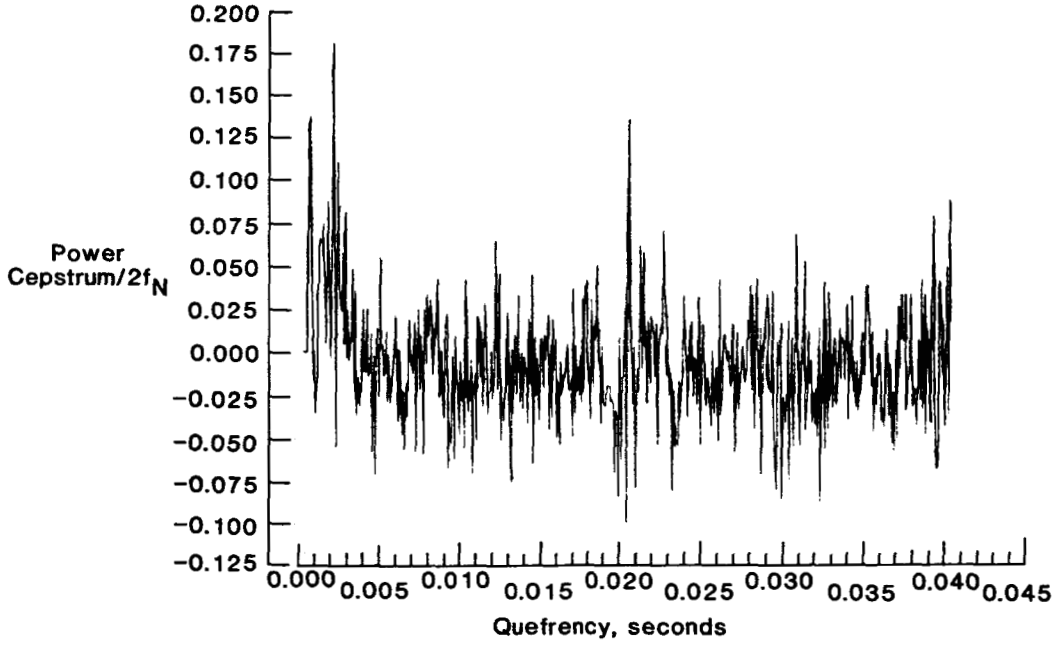

(b) Power cepstrum.

Figure 18.- Coefficient-averaged helicopter-rotor data of figure 16.

Standard Bibliographic Page

1. Report No.	2. Government Accession No.	3. Recipient's Catalog No.
NASA TP-2586		

4. Title and Subtitle	5. Report Date
Power Cepstrum Technique With Application to Model Helicopter Acoustic Data	June 1986
	6. Performing Organization Code: 505-61-51-06
7. Author(s): R. M. Martin and C. L. Burley	8. Performing Organization Report No.: L-16070
	10. Work Unit No.
9. Performing Organization Name and Address: NASA Langley Research Center, Hampton, VA 23665-5225	11. Contract or Grant No.
	13. Type of Report and Period Covered: Technical Paper
12. Sponsoring Agency Name and Address: National Aeronautics and Space Administration, Washington, DC 20546-0001	14. Sponsoring Agency Code

15. Supplementary Notes

R. M. Martin: Langley Research Center, Hampton, Virginia.
C. L. Burley: PRC Kentron, Inc., Hampton, Virginia.

16. Abstract

The application of the power cepstrum to measured helicopter-rotor acoustic data is investigated. A previously applied correction to the reconstructed spectrum is shown to be incorrect. For an exact echoed signal, the amplitude of the cepstrum echo spike at the delay time is linearly related to the echo relative amplitude in the time domain. If the measured spectrum is not entirely from the source signal, the cepstrum will not yield the desired echo characteristics and cepstral aliasing may occur because of the effective sample rate in the frequency domain. The spectral analysis bandwidth must be less than one-half the echo ripple frequency or cepstral aliasing can occur. The power cepstrum editing technique is a useful tool for removing some of the contamination because of acoustic reflections from measured rotor acoustic spectra. The cepstrum editing yields an improved estimate of the free field spectrum, but the correction process is limited by the lack of accurate knowledge of the echo transfer function. An alternate procedure, which does not require cepstral editing, is proposed which allows the complete correction of a contaminated spectrum through use of both the transfer function and delay time of the echo process.

17. Key Words (Suggested by Author(s))	18. Distribution Statement
Cepstrum analysis Acoustic reflections Echo removal Rotor acoustics Power cepstrum	Unclassified - Unlimited Subject Category 71

19. Security Classif. (of this report)	20. Security Classif. (of this page)	21. No. of Pages	22. Price
Unclassified	Unclassified	68	A04

For sale by the National Technical Information Service, Springfield, Virginia 22161